



HAL
open science

Climatic control on the retreat of the Laurentide Ice Sheet margin in easternmost Québec–Labrador (Canada) revealed by cosmogenic nuclide exposure dating

Pierre-Olivier Couette, Jean-françois Ghienne, Patrick Lajeunesse, Jérôme van der Woerd

► To cite this version:

Pierre-Olivier Couette, Jean-françois Ghienne, Patrick Lajeunesse, Jérôme van der Woerd. Climatic control on the retreat of the Laurentide Ice Sheet margin in easternmost Québec–Labrador (Canada) revealed by cosmogenic nuclide exposure dating. *Journal of Quaternary Science*, 2023, 38 (7), pp.1044-1061. 10.1002/jqs.3525 . hal-04256549

HAL Id: hal-04256549

<https://hal.science/hal-04256549v1>

Submitted on 24 Oct 2023

HAL is a multi-disciplinary open access archive for the deposit and dissemination of scientific research documents, whether they are published or not. The documents may come from teaching and research institutions in France or abroad, or from public or private research centers.

L'archive ouverte pluridisciplinaire **HAL**, est destinée au dépôt et à la diffusion de documents scientifiques de niveau recherche, publiés ou non, émanant des établissements d'enseignement et de recherche français ou étrangers, des laboratoires publics ou privés.

1 **Climatic control on the retreat of the Laurentide Ice Sheet margin in easternmost Québec-**
2 **Labrador (Canada) revealed by cosmogenic nuclide exposure dating**

3
4
5 **Pierre-Olivier Couette** ^{1,2,*}, **Jean-François Ghienne** ², **Patrick Lajeunesse** ¹, **Jérôme van der**
6 **Woerd** ²

7
8 ¹ *Département de Géographie, Université Laval, Québec, G1V 0A6, Canada*

9 ² *Institut Terre & Environnement de Strasbourg (ITES), UMR 7063, CNRS—Université de Strasbourg, France*

10
11 * Corresponding author E-mail address: pierre-olivier.couette.1@ulaval.ca

12
13 Jean-François Ghienne (ghienne@unistra.fr)

14 Patrick Lajeunesse (patrick.lajeunesse@ggr.ulaval.ca)

15 Jérôme van der Woerd (jerome.vanderwoerd@unistra.fr)

16
17
18
19 The authors declare that they have no known competing financial interests or personal
20 relationships that could have appeared to influence the work reported in this paper.

21 **ABSTRACT**

22 The Laurentide Ice Sheet was the largest ice sheet in the Northern Hemisphere during the
23 last glacial cycle. The effects of its demise on global climate and sea level changes during the
24 subsequent deglaciation are unequivocal. Understanding the interplay between ice sheets and
25 long-term or shorter term (e.g., abrupt) climatic events is therefore crucial for predicting future
26 rates of ice sheet melting and their potential contribution to sea level changes. Here, we present
27 37 new ¹⁰Be surface exposure ages from easternmost Québec-Labrador that allow identifying
28 close ties between regional deglaciation history and climate. These results reveal that the
29 Laurentide Ice Sheet disconnected from the Newfoundland Ice Cap by ~14.1 ka. Samples
30 collected from moraine boulders indicate that this event was followed by the occurrence of five
31 major stillstands and/or readvance stages of the Laurentide Ice Sheet margin. Integrating our new
32 moraine ages to those of earlier studies allows depicting a temporal framework including events
33 at ~12.9 ka, ~11.5 ka, ~10.4 ka, ~9.3 ka and ~8.4-8.2 ka. These moraine ages highlight a strong
34 sensitivity of the LIS to temperature changes in the Northern Hemisphere, as the documented
35 continental ice margin stabilizations coincide with abrupt cooling events recorded in Greenland
36 ice cores. These observations support the idea of a negative feedback mechanism induced by
37 meltwater forcings into the North Atlantic Ocean which, in turn, provoked repeated cold
38 reversals during the Younger Dryas and early Holocene.

39

40

41 **Keywords:** Laurentide Ice Sheet; Deglaciation; Moraines; Cosmogenic ¹⁰Be exposure dating;
42 Abrupt climatic events; Québec-Labrador

43 **Introduction**

44 The ice sheets that once covered the Northern Hemisphere played an undeniable role in
45 modulating global changes since the Last Glacial Maximum (LGM), as their growth and decay
46 were closely interconnected with atmospheric/oceanic circulation and sea-level changes (Alley et
47 al., 1997; Clark et al., 2000; Carlson et al., 2008; Denton et al., 2010; Briner et al., 2020; Lowell
48 et al., 2021). Warming temperature during the deglaciation that followed the LGM provoked
49 enhance freshwater inputs into the North Atlantic Ocean, slowing the Atlantic Meridional
50 Overturning Circulation (AMOC) and ultimately reducing air temperature over the Northern
51 Hemisphere (Barber et al., 1999; Fisher et al., 2002; McManus et al. 2004; Rohling and Pälike,
52 2005; Carlson and Clark, 2012; Jennings et al., 2015; Süfke et al., 2022). The interplay between
53 such feedbacks and ice mass evolutions is still, however, poorly constrained, as Holocene
54 climate evolution and its sensitivity to known forcings remain in some cases elusive (Axford et
55 al., 2009; Jennings et al., 2015; He and Clark, 2022). Documenting the response of former ice
56 sheets – such as the Laurentide Ice Sheet (LIS) – to external forcing, and the timing of this
57 response, is critical for assessing the contribution of melting ice masses to past and future sea-
58 level rise.

59 The study of stillstands and readvances of the LIS margin during its overall retreat
60 provide key information on late Wisconsinan and early Holocene climate fluctuations, which is
61 essential for (i) improving our knowledge on long-term glacial and deglaciation history of former
62 ice sheets, (ii) determining their sensitivity to climate change and (iii) identifying trigger
63 mechanisms of ice margin behaviour (Lesnek and Briner, 2018; Briner et al., 2020; Young et al.,
64 2020). Identification of causes, such as drainage of large glacial lakes, contribute in assessing
65 their potential role in, and response to millennial-scale abrupt climatic events (e.g., Fisher et al.,

66 2002; Lajeunesse et al., 2008; Yu et al., 2010; Dubé-Loubert et al., 2018; Leydet et al., 2018;
67 Brouard et al., 2021; Süfke et al., 2022). Dating and reconstructing the evolution of former ice
68 sheet margins is therefore crucial for understanding the long-term interconnections between ice
69 sheets and the global climate system and identifying the interfering feedback mechanisms that
70 influence deglaciation (Briner et al., 2020; Lowell et al., 2021).

71 The development of cosmogenic exposure dating has contributed substantially to
72 improving reconstructions of the deglacial history in North America by allowing direct dating of
73 landforms deposited during stagnation or retreat stages of ice margins (Balco, 2020). Over the
74 last decades, an ever growing number of studies focused on identifying and dating major
75 stillstands and readvances of the LIS margin during its retreat following the LGM (i.e., Marsella
76 et al., 2000; Clark et al., 2003; Briner et al., 2005, 2007, 2009; Balco et al., 2009; Young et al.,
77 2012, 2020, 2021; Bromley et al., 2015; Davis et al., 2015; Ullman et al., 2016; Margreth et al.,
78 2017; Crump et al., 2020; Lowell et al., 2021). However, as these studies mostly focused on
79 specific sectors of the LIS, large geographical gaps in available absolute ages on glacial
80 landforms remain, especially at its eastern fringe. Despite the relatively large number of
81 radiocarbon ages available in southern Labrador and adjacent easternmost Québec that provide
82 minimum-limiting ages for deglaciation (i.e., King, 1985; Dyke et al., 2003; Dalton et al., 2020),
83 the chronology of most of the major moraine systems marking stabilizations/readvances of the
84 retreating LIS margin in the region is still poorly constrained.

85 In this paper, we report on the deglaciation history of the eastern sector of the LIS by
86 using terrestrial cosmogenic ^{10}Be exposure dating of boulders from major moraine systems. This
87 chronological dataset coupled with previously published and new radiocarbon ages allow (1)
88 constraining the position of ice margin during its retreat; and (2) assessing retreat rates of the ice

89 margin in order to identify time intervals of important changes. These results provide a revised
90 deglacial chronological framework across five former ice marginal stillstand/readvances
91 positions along a 500-km-long transect from the coast to the Labrador hinterland. These results
92 allow discussing the potential causes for deposition of moraines in easternmost Québec-Labrador
93 and their implication for regional climate.

94 **Regional setting**

95 Easternmost Québec-Labrador (Canada) host a series of moraines marking the overall
96 retreat of the LIS during the late-glacial and early Holocene (Fig. 1). The region lies within the
97 Grenville geological province of the Canadian Shield and is underlain mainly by Proterozoic
98 quartzofeldspathic gneisses, granites and anorthosites (Greene, 1974; Hynes and Rivers, 2010).
99 Regional physiography consists of a hilly ‘peneplain’ ranging from 300 to 500 m in elevation
100 that is deeply incised by structural valleys. The study area also includes the Lake Melville
101 depression, an estuary that stretches 200 km inland from the Atlantic coast, and the Mealy
102 Mountain Massif, a prominent plateau-topped highland reaching over 1000 m. Except for the
103 area located to the northwest of Lake Melville, the study area is characterized by a generally thin
104 ice-contact cover of deposits and valleys partially filled with glaciomarine to glaciofluvial
105 deposits (Fulton and Hodgson, 1979; King, 1985). Five extensive morainic systems (>100 km
106 long) previously identified in easternmost Québec-Labrador represent major successive positions
107 of the retreating LIS margin following the late Wisconsin glacial cycle (i.e., from SE to NW:
108 Brador, Belles Amours, Paradise, Little Drunken and Sebaskachu moraine systems: Fulton and
109 Hodgson, 1979; King, 1985; Occhietti et al., 2011). Although these moraines undeniably
110 represent mappable, regional-scale stillstands and/or potential readvances of the LIS margin,
111 their age remains poorly constrained and their correlations with other sectors of the LIS to the

112 North (e.g., Baffin Island) or to the West (e.g., St. Lawrence estuary) are still debated (e.g., King
113 et al., 1985; Grant, 1992; Occhietti et al., 2011).

114 Early workers proposed that easternmost Québec-Labrador was not covered by the LIS
115 during the late Wisconsinan glaciation (Coleman, 1921). The idea of a restricted LIS in the
116 region was later invoked: some authors positioned the LIS margin at the LGM at the Brador
117 Moraine near the present coastline (Ives, 1978; Vilks and Mudie, 1978) and others suggested that
118 it was located even more inland at the Paradise Moraine based on the scarcity of
119 geomorphological evidence further east (Fig. 1; Fulton and Hodgson, 1979). In more recent
120 investigations, several authors revised this restricted position by demonstrating that the LIS
121 completely covered southern Labrador at the LGM, reaching as far as the shelf edge in Hawke
122 Trough and on Hamilton Banks (Josenhans et al., 1986; Piper, 1991; Grant, 1992; Roger et al.,
123 2013). After its separation from the Newfoundland Ice Cap, the LIS margin stabilized at a
124 position located at the modern coast of eastern Québec-Labrador, depositing the Brador and the
125 Belles Amours moraine systems (Fig. 1; Grant, 1992). The age of the Brador and the Belles
126 Amours moraine systems were estimated at 12.5 ^{14}C ka BP (~15 cal ka BP) and 11.0 ^{14}C ka BP
127 (~13 cal ka BP), respectively (King, 1985). Grant (1992) proposed that the LIS margin stabilized
128 when it grounded at marine limit to build the Brador Moraine at 12.6 ^{14}C ka BP (~15 cal ka BP)
129 and deposited the Belles Amours Moraine shortly after (<200 years) in the frame of a regional
130 readvance. The ice margin then retreated westward and deposited successively the Paradise and
131 Little Drunken moraine systems during two stillstands and/or readvances of the LIS margin
132 (King, 1985). The Paradise Moraine was proposed to correspond to the early Younger Dryas
133 (YD) event, therefore correlating to the St-Narcisse Moraine of southern Québec (Dyke and
134 Prest, 1987; King, 1985; Grant, 1992; Occhietti, 2007), while the Little Drunken Moraine was

135 speculated to correspond to the Québec North Shore Moraine deposited at ~10.8 ka BP (Dubois
136 and Dionne, 1985; Dietrich et al., 2019). However, the abandonment of the Paradise Moraine
137 and Québec North Shore Moraine have been recently dated at 10.3 ± 0.6 ka and 9.2 ± 0.5 ka,
138 respectively, using cosmogenic exposure dating (Ullman et al., 2016). After this stage of the
139 deglaciation, the LIS margin stabilized again at the west end of Lake Melville and deposited the
140 Sebaskachu Moraine. The Little Drunken Moraine has been tentatively correlated to the
141 Sebaskachu Moraine by several authors (i.e., Blake, 1956; Fulton and Hodgson, 1979; Occhietti
142 et al., 2011), although no formal geomorphological connection has been observed between the
143 two systems. The ice margin is estimated to have retreated from the Sebaskachu position at 8.0
144 ^{14}C ka BP (~8.8 cal ka BP) and reached central Labrador by 7.0 ^{14}C ka BP (~7.8 cal ka BP; King,
145 1985). Similarly, cosmogenic exposure dating on erratic boulders yielded ages of $8.6 \text{ ka} \pm 0.6 \text{ ka}$
146 west of Lake Melville and $7.5 \text{ ka} \pm 0.4 \text{ ka}$ for central Labrador (Ullman et al., 2016). Ice retreat
147 then took place rapidly with a final ablation of the LIS at ~5.5 ^{14}C ka BP (~6.0 cal ka BP) over
148 the central Québec-Labrador Peninsula (Richard et al., 1982; Clark et al., 2000; Jansson, 2003;
149 Occhietti et al., 2011; Dubé-Loubert et al., 2018), leaving series of small recessional moraines
150 across the landscape.

151 **Methods**

152 **Field mapping and sampling**

153 Positions of the former margins (i.e., moraines) of the LIS were mapped in order to
154 spatially constrain its successive extents during deglaciation of the easternmost Québec-Labrador
155 sector. Our mapping builds upon previous investigations on moraines across the study area that
156 was, however, sporadic and not sufficiently constrained in some sectors (Dubois and Dionne,
157 1985; Grant, 1992; Klassen et al., 1992). Interpretation of Landsat satellite imagery allowed

158 refining and extending previous maps of moraine deposits. All mapped moraine systems were
159 then visited in the field and sampled. Additionally, the chronology (^{10}Be and ^{14}C) was used for
160 interpolating ice margin positions in areas lacking well-preserved moraine deposits.

161 Surface exposure ages on moraine boulders, erratics and bedrock outcrops were obtained
162 using cosmogenic beryllium-10 dating (from here on referred to as ^{10}Be ; Fig. 2). ~1 kg of rock
163 were collected from the upper 2 cm of boulder surfaces using a handheld rocksaw, a hammer and
164 a chisel. The flat top of stable boulders embedded in the moraine matrix were targeted to
165 minimize overturning possibility, post-deposition exhumation and extreme weathering. Where
166 available, quartz veins or quartz-rich material were extracted from the boulders. Samples were
167 precisely documented in the field, including site description, coordinates and elevation obtained
168 from a handheld GPS.

169 **Sample preparation and analysis**

170 Samples were processed at the cosmogenic nuclide laboratory at the University of
171 Strasbourg following a well-established protocol modified from Kohl & Nishiizumi (1992) and
172 Bierman et al. (2002). All samples were crushed and sieved to isolate the 250-1000 μm fraction,
173 which was subsequently treated by leaching in an HCl solution to eliminate oxides and organic
174 material. Up to nine ultrasonic leaching cycles with diluted HF and HNO_3 (~1% each) solution
175 were needed to purify the quartz. A commercial ^9Be carrier (~0.25-0.5 mg) was added to the
176 samples before dissolving the pure quartz in concentrated HF (48%) and HNO_3 (68%).
177 Beryllium was isolated through anion and cation exchange columns and then precipitated as
178 hydroxide. Beryllium hydroxide was dried and calcinated to BeO at 750°C . $^{10}\text{Be}/^9\text{Be}$ ratios were
179 measured at ASTER, the French Accelerator Mass Spectrometry (AMS) at CEREGE (Aix-en-
180 Provence). The measurements of samples were normalized against an in-house CEREGE

181 standard STD11, with an assumed $^{10}\text{Be}/^9\text{Be}$ ratio of $(1.191 \pm 0.013) \times 10^{-11}$ (Braucher et al.,
182 2015) and a ^{10}Be half-life of 1.387 ± 0.012 Ma (Chmeleff et al., 2010; Korschinek et al., 2010).
183 A procedural blank was processed with each batch of samples to evaluate ^{10}Be contamination
184 during laboratory procedures. Blank $^{10}\text{Be}/^9\text{Be}$ ratios range from $5.21 \pm 0.42 \times 10^{-15}$ to 6.12 ± 0.45
185 $\times 10^{-15}$; average blank $^{10}\text{Be}/^9\text{Be}$ ratios were $5.74 \pm 0.59 \times 10^{-15}$ ($n = 8$) (Table 1).

186 **^{10}Be age calculations**

187 ^{10}Be ages were calculated using the online exposure age calculator formerly known as the
188 CRONUS-Earth online exposure age calculator version 3.0 (Balco et al., 2008;
189 <https://hess.ess.washington.edu/>). Calibration was done using the northeastern North America
190 (NENA) ^{10}Be production rate of 4.04 ± 0.27 atoms/g/a (Balco et al., 2009) and the nuclide- and
191 time-dependent LSDn scaling scheme (Lifton et al., 2014). The NENA production rate is
192 statistically identical to other high latitude production-rate calibration datasets such as the Baffin
193 Bay (Young et al., 2013) and the Rannoch Moor (Putnam et al., 2019) production rates. For
194 comparison, the global production rate (Borchers et al., 2016) would result in ages that are ~5%
195 younger. By comparison, using the St or Lm scaling schemes (Lal, 1991; Stone, 2000) would
196 result in exposure ages that are ~5% older than the LSDn-derived ^{10}Be ages. The effects of
197 postglacial erosion on ^{10}Be ages were neglected as sampled bedrock and boulder surfaces
198 commonly displayed glacial striations, suggesting little surface erosion since deglaciation.
199 Topographic shielding was not taken into account for boulders and sampled surfaces as it was
200 estimated negligible (<1%). Post-glacial isostatic uplift corrections were not accounted for in the
201 final results (Supplementary Material; Table S1), as the effects of glacio-isostatic rebound on
202 cosmogenic nuclides production are not well constrained (Balco et al., 2009; Young et al.,
203 2020b). Snow cover corrections were also omitted in the calculation of the ages as we sampled

204 boulders located on top of moraine crests, which are often wind-swept and thus likely prevented
205 any significant snow accumulation (Supplementary Material; Table S2). Individual ^{10}Be
206 exposure ages are presented with 1σ uncertainty (Table 1). Stated uncertainties are analytical
207 only. Outliers were identified using the CRONUS-Earth online calculator and defined as ^{10}Be
208 ages that are $>2\sigma$ older or younger from the mean of the remaining ^{10}Be ages. Probability
209 distribution function (PDF) plots were generated using the iceTEA (Tools for Exposure Ages
210 from ice margins; <http://ice-tea.org/en/>) “Import and plot ages” tool (Jones et al., 2019), in which
211 the moraine ages were defined as the error-weighted mean of the sample population and the
212 error-weighted internal uncertainty, excluding outliers. We include the production rate
213 uncertainty in quadrature when comparing and discussing landform ages with independent
214 climate records and radiocarbon ages. Additionally, ^{10}Be ages from Ullman et al. (2016) were
215 recalculated using the same parameters as above to allow direct comparison with our new ^{10}Be
216 ages (Supplementary Material; Table S3).

217 **Radiocarbon dating**

218 Accelerator Mass Spectrometry (AMS) radiocarbon dating was carried out on marine
219 shells collected in 2019. The four obtained AMS ^{14}C ages were calibrated within the age-depth
220 modelling process and converted to calendar years using the online software Calib 8.2 (Stuiver
221 and Reimer, 1993; <http://calib.org/>) with the Marine20 radiocarbon age calibration curve (Heaton
222 et al., 2020). A local reservoir correction (ΔR) of -2 ± 69 was used to account for the regional
223 offset of the world ocean ^{14}C age (McNeely et al., 2006). These four ages complement a dataset
224 of 41 previously published ^{14}C ages that have also been recalibrated. Marine samples were
225 calibrated using the aforementioned parameters, whereas terrestrial samples were calibrated
226 using the IntCal20 radiocarbon age calibration curve (Reimer et al., 2020). All individual

227 radiocarbon ages are presented as the mean of the calibrated age range with 1σ uncertainty
228 (Table 2).

229 **Retreat rates**

230 The moraine map was used to reconstruct retreat rates of the LIS in easternmost Québec-
231 Labrador. When ice-contact deposits were absent (i.e., west of Lake Melville), retreat isochrones
232 of former ice margin positions (i.e., 7.9, 7.6 and 7.5 ka) were tentatively drawn perpendicular to
233 the ice-flow direction where minimum limiting ages are available. Ice retreat rates were then
234 calculated along time-distance transects perpendicular to the retreating ice margin. The transects
235 were hand-drawn radially from the ~7.5 ka isochron of the LIS to the coast, where they are at
236 intervals of ~50 km. This approach allowed to cross each moraine system at least three times,
237 since no transect intersects all five mapped ice margin positions. The mean linear retreat rate was
238 then calculated between every ice margin position using the ages for each moraine system
239 presented in this paper for estimating the land-based ice margin retreat. These retreat rates
240 represent minimum values as they do not take into account possible readvances of the LIS
241 margin and their respective durations.

242 **Results**

243 **^{10}Be ages and moraine systems**

244 Moraine systems along the SE to NW transect of eastern Québec-Labrador are here
245 briefly described. The resulting ^{10}Be ages from the sampled boulders and surfaces are provided
246 for each of these moraine systems.

247 Three erratic boulders located above marine limit were sampled in the easternmost sector
248 of the study area, where morainic landforms are sparse. These erratic boulders constrain a series
249 of closely spaced recessional moraines that have not yet been linked to any major moraine

250 system. Since the moraine ridges were mostly located below marine limit, three boulders –
251 located on both sides – were selected to assess the timing of their formation; two ‘coastal’
252 boulders (LBD19-30 and LBD19-31) were located within 2 km of the coast and one ‘inland’
253 boulder (LBD19-28) was sampled ~40 km from the coast. The coastal erratic boulders provided
254 ^{10}Be ages of 14.1 ± 0.6 and 12.5 ± 0.5 ka (Table 1), whereas the erratic boulder collected 40 km
255 inland provided a ^{10}Be age of 12.0 ± 0.5 ka (Table 1).

256 The Brador Moraine consists of small-amplitude moraine ridges coinciding with the
257 marine limit (~140 m) (Fig. 3A) and outwash deposits occupying lower areas in narrow valleys.
258 Some moraine ridges show traces of local glaciotectonic deformation, indicating readvance of
259 the ice margin before stabilization. Five boulders were sampled from three different segments of
260 the Brador Moraine over a distance of ~75 km. These boulders yielded consistent ^{10}Be ages
261 ranging between 12.6 ± 0.7 and 13.4 ± 0.5 ka and a weighted average of 12.9 ± 0.2 ka (Table 1;
262 Fig. 4).

263 The Belles Amours Moraine consists of series of small sinuous ridges, each a few meters
264 high and less than 20 m wide (Fig. 3B). This moraine system has a SW-NE orientation and is
265 cross-cutting the Brador Moraine west of Blanc Sablon (Fig. 1). Five boulders were sampled
266 from two of the main crests of the Belles Amours Moraine. They yield ^{10}Be ages ranging from
267 11.2 ± 0.5 to 12.0 ± 0.4 ka (Table 1), resulting in a weighted average of 11.5 ± 0.3 ka (Fig. 4).
268 Additionally, a bedrock surface sampled 4 km behind the Belles Amours Moraine and at 75
269 meters above sea-level (m.a.s.l.) – located below marine limit (~130 m.a.s.l.; Grant, 1992) –
270 yielded an age of 10.8 ± 0.4 ka (LBD19-46; Table 1), indicating the emergence from marine
271 waters and hence representing a minimum-limiting age constraint.

272 The Paradise Moraine consists of a 20 km-wide complex of glaciofluvial deposits pitted
273 with kettles, as well as fields of hummocky and ribbed moraines (Fig. 3C). East of the Mealy
274 Mountains, the moraine overprints glacial lineations at an odd angle, testifying an ice flow
275 reorganization that suggests an ice margin readvance. Five samples were collected in the
276 Paradise Moraine and yielded a large range of ages from 11.4 ± 0.4 to 37.1 ± 1.2 ka (Table 1).
277 Two samples yielded (too-) old ^{10}Be ages of 20.8 ± 0.7 and 37.1 ± 1.2 ka, while the three
278 remaining samples have exposure ages ranging from 11.4 ± 0.4 to 12.7 ± 0.5 ka and a resulting
279 weighted average of 12.1 ± 0.6 ka (Fig. 4).

280 The Little Drunken Moraine is located ~250 km inland from the coast. It has a lobate
281 geometry and is defined by series of 5 to 40 m-high till ridges (Fig. 3D) associated to extensive
282 outwash-plain deposits in proglacial valleys. Five samples were collected from the main crest of
283 the Little Drunken Moraine: three samples yielded ^{10}Be ages ranging from 9.8 ± 0.4 to 11.3 ± 0.4
284 ka, with two ages at 13.5 ± 0.4 and 14.7 ± 0.5 ka considered as outliers (Table 1). The weighted
285 average of the three remaining ages is 10.6 ± 0.7 ka (Fig. 4).

286 Two bedrock surfaces were sampled from the top of Mokami Hill (488 m.a.s.l.; Fig. 1) in
287 order to assess ice thinning at the head of Lake Melville (LBD19-74 and LBD19-75). Although
288 located less than 50 m apart, these sampled yielded disparate ^{10}Be ages of 10.0 ± 0.4 and $13.8 \pm$
289 0.5 ka (Table 1). Dating surfaces from the mountain top west of Lake Melville therefore remains
290 inconclusive. The large span of the ages (> 3 ka) suggests that 1) at least one sample is
291 unreliable, or 2) they have endured differential erosion. Although it is likely that the older age is
292 unreliable based on its location and nearby ages (i.e., the Sebaskachu Moraine), it is impossible
293 to assess the actual exposure age of the mountain surface at this point and more samples should
294 be collected to document the thinning of the LIS in the region during the early Holocene.

295 The Sebaskachu Moraine, located west of Lake Melville, consists of small linear
296 moraines with well-defined narrow crests of ~10 m high on the plateau (Fig. 3E); in valleys it
297 consists of large (>50 m) subaqueous ice-contact depositional systems. Five boulders sampled
298 from the Sebaskachu Moraine on the plateau yielded ^{10}Be ages ranging between 7.9 ± 0.3 to 9.1
299 ± 0.3 ka (Table 1). The weighted average of these five samples is 8.4 ± 0.4 ka (Fig. 4).
300 Additionally, a boulder was sampled from the top of a valley moraine in North West River at 65
301 m.a.s.l. and yielded an age of 7.8 ± 0.4 ka (LBD19-84; Table 1). This site – located below
302 marine limit (~135 m.a.s.l.; Fitzhugh, 1973) – provides timing of the emergence rather than ice
303 retreat. The regional relative sea-level curve from Fitzhugh (1973) suggests that the sample was
304 shielded by the water column for up to 600 years. It therefore only provides a minimum estimate
305 of the deglaciation, although adding these 600 years would closely match the weighted age
306 calculated for the Sebaskachu Moraine.

307 Five samples were also collected 40 km west of Happy Valley-Goose Bay on minor
308 moraine ridges (< 3m) in the Peter's River valley, above the marine and lake limits. The samples
309 yielded three ^{10}Be ages ranging from 7.5 ± 0.3 to 9.0 ± 0.4 ka, with two outliers at 6.8 ± 0.4 and
310 12.4 ± 0.5 ka (Table 1). The three remaining samples are, however, slightly disparate with a ^{10}Be
311 weighted average age of 8.1 ± 0.5 ka (Fig. 4).

312 **Radiocarbon ages**

313 Three shell samples were collected in the southern extension of the Sebaskachu moraine,
314 near North West River. These shells were embedded within the till composing the subaqueous
315 ice-contact system, therefore possibly pre-dating readvance of the ice margin. These samples
316 yielded consistent ages of 8.5 ± 0.1 cal ka BP (LBD19-62), 8.5 ± 0.1 cal ka BP (LBD19-61) and
317 8.1 ± 0.2 cal ka BP (LBD19-81). A shell collected in glaciomarine muds of the Churchill River

318 bank 50 km west of the Sebaskachu Moraine yielded an age of 8.2 ± 0.2 cal ka BP (LBD19-79).
319 Together, these results provide maximum and minimum limiting ages for the deposition of the
320 Sebaskachu Moraine, which are in agreement with (i) former ^{14}C dating (Fig. 5; Table 2), (ii) the
321 cosmogenic exposure age of the Sebaskachu Moraine (8.4 ± 0.4 ka).

322 **Discussion**

323 **Ice margin stabilizations in easternmost Québec-Labrador and regional correlations**

324 The new cosmogenic exposure ages allow defining the timing of deposition of the
325 moraine systems of easternmost Québec-Labrador that record major readvance and/or
326 stabilization stages of the LIS margin during its overall northwestward retreat. These results are
327 consistent and in chronological order in most cases, except for the Paradise Moraine that appears
328 older than the Belles Amours Moraine deposited ~ 100 - 120 km to the east. The timing and
329 correlations of the moraine systems are discussed below with respect to previously published
330 data.

331 The age of the Brador Moraine system at 12.9 ± 0.2 ka is supported by a robust ^{10}Be
332 chronology and corresponds to the beginning of the YD chronozone. This age is further
333 supported by a series of minimum-limiting radiocarbon ages ranging from 11.4 ± 0.1 to $12.2 \pm$
334 0.2 cal ka BP and maximum-limiting ages ranging from 12.7 ± 0.2 to 13.0 ± 0.2 cal ka BP (Fig.
335 5; Table 2). Additionally, the inland erratic boulder dated at 12.0 ± 0.5 ka, supported by a nearby
336 age of 12.4 ± 0.1 cal ka BP (Engstrom and Hansen, 1985; Fig. 5; Table 2), suggests that the
337 recessional moraine system located between the two erratic boulder sites ('coastal' and 'inland')
338 may correspond to or slightly succeed the Brador Moraine. There is no indication, however, for
339 its extension north of this sector, but it is highly probable that it is located beyond the coast of
340 southeastern Labrador as foraminifera samples offshore yielded ages ranging from 11.1 ± 0.2 to

341 12.3 ± 0.3 cal ka BP (Table 2). Our results therefore suggest that the Brador Moraine is time-
342 equivalent to the St-Narcisse Moraine in southern Québec (Occhietti, 2007) and possibly to one
343 of the ice-contact grounding-zone wedge systems observed offshore the Québec North Shore
344 region (Lajeunesse et al., 2019). It would also be contemporaneous to the Saglek Moraine
345 located in the Torngats Mountains of northern Labrador (Clark et al., 2003). Consequently, the
346 coastal erratic boulders suggest deglaciation of the coast of easternmost Québec-Labrador
347 between 14.1 ± 0.6 and 12.5 ± 0.5 ka. The opening of the Belle Isle Strait and isolation of the
348 Newfoundland Ice Cap from the LIS therefore occurred prior to that timing, presumably during
349 the Bølling–Allerød warm period (14.7-12.9 ka BP). This interpretation supports what has
350 previously been proposed by Shaw et al. (2006) who argued that disconnection between the two
351 ice masses occurred between 14.8 and 14.0 cal ka BP. In this scheme, the time frame proposed
352 by Grant (1992) appears to be erroneous, as they argued that the opening of the Strait of Belle
353 Isle and separation of the two ice masses occurred prior to 15 cal ka BP.

354 The age of 11.5 ± 0.3 ka for the deposition of the Belles Amours moraine ridges indicates
355 a stabilization of the LIS margin at the beginning of the Holocene or near the end of the YD.
356 This timing for the deposition of the Belles Amours moraine system contradicts the
357 interpretation of Grant (1992) who argued that their deposition may have taken place only a few
358 centuries after deposition of the Brador Moraine on the basis of only a minor relative sea-level
359 fall between the two events. However, a relatively stagnant ice margin during the YD and a
360 significant readvance – as evidenced by the cross-cutting relationship of the two moraines (Fig.
361 1) – may have significantly limited the rate of glacio-isostatic rebound in the region, similar to
362 observations in Greenland during the Neoglacial ice expansion (Long et al., 2009). Although the
363 mapped extent of this moraine is relatively limited (~100 km), the 12.0 ± 0.5 ka age of the inland

364 erratic suggests that the ice margin was probably located west of this site at the time of
365 deposition of the Belles Amours Moraine. Its northern extent can, however, only be tentatively
366 mapped. Additionally, a basal lacustrine sample dated at 11.5 ± 0.2 cal ka BP (Lamb, 1980; Fig.
367 5; Table 2) – similar to the mean cosmogenic exposure age of the Belles Amours Moraine
368 samples – may provide an indication for its approximate location near that site. The timing of
369 deposition of the Belles Amours Moraine suggests a correlation with the Mars-Batiscan Moraine
370 in southern Québec (Occhiatti, 2007), although the physical connection between the two systems
371 remains ambiguous. It is possible that the Belles Amours Moraine corresponds offshore to one of
372 the youngest ice-contact grounding-zone wedges (Lajeunesse et al., 2019) and, onshore, to the
373 Baie Trinité Moraine on the Québec North Shore (Fig. 1B; Occhiatti et al., 2011). However,
374 further dating would be needed to confirm the correlation as the timing of deposition of the Baie-
375 Trinité Moraine is still not well constrained.

376 Direct dating of the Paradise Moraine remains inconclusive. Two of the samples yielded
377 ages >20 ka, while the three remaining sample yielded an average age of 12.1 ± 0.6 ka. This age
378 is stratigraphically problematic as it is older than the Belles Amours Moraine. Dated boulders
379 located west of the Paradise Moraine system yielded a mean age of 10.4 ± 0.6 ka (Ullman et al.,
380 2016) or 9.4 ± 0.8 ka when recalculated using the same parameters as for our ^{10}Be ages
381 (Supplementary Table 3; Fig. 5). Interestingly, four samples from Ullman et al. (2016) also
382 yielded erroneous and largely too old ages (site CL1B in the original publication). The
383 abundance of old ages implies that boulder recycling was important during the deposition of the
384 Paradise Moraine. It is, however, uncertain where these boulders came from and when they were
385 first exhumed. Similarly, the dating of lake sediments, from about 50 km east of the moraine,
386 yielded ^{14}C ages ranging to > 30 cal ka BP (Lamb, 1978) and were interpreted as the result of

387 contamination by old carbon (King, 1985). These different occurrences of ages > 20 ka suggest
388 that the boulders sampled from the Paradise Moraine were affected by isotopic inheritance
389 yielding artificially old and erroneous exposure ages. This isotopic inheritance points toward
390 generally low glacial erosion rates and/or transport of supraglacial material on the plateau south-
391 west of the Mealy Mountains. However, an age of 9.4 ± 0.1 cal ka BP (King, 1985; Fig. 5; Table
392 2) collected from basal lake sediments 20 km west of the moraine provide an indication for a
393 later deglaciation. A moraine system located east of the Mealy Mountains correlates to the
394 Paradise Moraine and corresponds to a lobe emanating from Lake Melville, leaving the summits
395 of the Mealy Mountains deglaciated at that time. Radiocarbon dating of marine shells along a
396 riverbank east of this moraine system yielded ages ranging from 9.2 ± 0.2 to 9.6 ± 0.3 cal ka BP
397 (Hodgson and Fulton, 1972; Fig. 5; Table 2), which is in line with the exposure age retained for
398 the abandonment of the Paradise Moraine at 9.4 ± 0.8 ka (recalculated from Ullman et al. 2016).
399 Correlations with other sectors of the Québec-Labrador Dome is challenging at this stage as the
400 extension of the Paradise Moraine beyond the study area remains elusive.

401 The Little Drunken Moraine cosmogenic exposure ages also show a wide distribution
402 with two outliers. These results should be interpreted with caution since they were also collected
403 from a site on the plateau south-west of the Mealy Mountains; these samples were therefore
404 potentially subject to isotopic inheritance similarly to the Paradise Moraine samples.
405 Nonetheless, the resulting weighted mean of 10.6 ± 0.7 ka matches the ^{14}C ages for the Québec
406 North Shore Moraine, which has been previously mapped as the southwestern extension of the
407 Little Drunken Moraine (Dubois and Dionne, 1985; Dietrich et al., 2019). In turn, recent
408 cosmogenic dating of the Québec North Shore Moraine suggested a ^{10}Be age of 9.2 ± 0.5 ka for
409 its abandonment (Ullman et al., 2016). Recalculation of these ages again gives an even younger

410 moraine age of 8.5 ± 0.7 ka. Regardless of the calculation method, ages from Ullman et al.
411 (2016) are consistent with a radiocarbon age of 9.3 ± 0.1 cal ka BP (King, 1985; Fig. 5; Table 2)
412 collected from the base of a lacustrine record located less than 10 km northwest of the Little
413 Drunken Moraine. The extension of the moraine is arguably represented across Lake Melville
414 either on seismic data (Fig. 1C – M1; Syvitski and Lee, 1997) or on swath bathymetry imagery
415 (Fig. 1C – M2; Gebhardt et al., 2020). Which of these two moraines represents the Little
416 Drunken Moraine is unclear as the physical connection between these systems is missing. The
417 connection with an unnamed moraine system located north of Lake Melville (Fig. 1C – M3) –
418 interpreted to be equivalent to the Little Drunken Moraine by Batterson et al. (1987) – is also
419 absent. However, a minimum-limiting age of 8.8 ± 0.2 cal ka BP (Vilks et al., 1987; Fig. 5;
420 Table 2) on shells in Lake Melville indicate that the ice margin likely extended across the lake at
421 the time of the deposition of the Little Drunken Moraine. To the north, a moraine system of
422 similar age (Tasiuyak Moraine – 9.3 cal ka BP) reported in the Nain-Okak region could represent
423 the northern extension of the ice margin at the time of the deposition of the Little Drunken
424 Moraine (Andrews, 1963; Recq et al., 2020).

425 Cosmogenic exposure dating of the Sebaskachu Moraine yielded an age of 8.4 ± 0.4 ka,
426 which is in strong agreement with the radiocarbon ^{14}C ages ($< 8.4 \pm 0.1$ and $> 8.2 \pm 0.2$ cal ka
427 BP; Table 2) bracketing the moraine formation age. A shell collected in deglacial deposits on top
428 of the moraine in North West River further supports abandonment of the Sebaskachu Moraine by
429 8.3 ± 0.2 cal ka BP (Lowdon and Blake, 1980; Table 2). Additionally, shells collected from three
430 ice-contact deltas north of our sample site yield ages of 8.4 ± 0.1 cal ka BP, 8.2 ± 0.2 cal ka BP
431 and 8.2 ± 0.1 cal ka BP (Fig. 5; Table 2). As these deltas are all located downstream from lakes,
432 it is unlikely that their deposition correspond to stabilization of the ice margin further inland.

433 These ages allow confirming the northern extension of the Sebaskachu Moraine up to the
434 Adlatok Valley, where a ~20 km gap remained in the moraine mapping (Fig. 1C). The southern
435 extension of the moraine remains undefined, but minimum-limiting radiocarbon ages of 8.4 ± 0.1
436 cal ka BP and 8.3 ± 0.1 cal ka BP (King, 1985; Fig. 5; Table 2) collected in lake sediments
437 suggest that the ice margin at that time was likely located ~50 km west of the Little Drunken
438 Moraine. The age of the Sebaskachu Moraine correspond to the timing of deposition of the
439 extensive Sakami Moraine in western Québec (Hillaire-Marcel, 1981; Hardy, 1982; Lajeunesse
440 and Allard, 2003; Lajeunesse, 2008; Ullman et al., 2016) and the Cockburn moraines on Baffin
441 Island (Bryson et al., 1969; Andrews and Ives, 1978; Dyke, 1979; Miller, 1980; Briner et al.,
442 2007; Young et al., 2012).

443 The Peter's Moraine exposure age of 8.1 ± 0.5 ka is comparable to a nearby site from
444 Ullman et al. (2016), which gave an age of 7.7 ± 0.4 ka. The moraine age is similar to the age of
445 8.2 ± 0.2 cal ka BP on a shell collected in glaciomarine deposits along the Churchill River (Fig.
446 1; Table 2). It is also coeval with another shell collected in a nearby outcrop that yielded an age
447 of 8.2 ± 0.4 cal ka BP (Lowdon and Blake, 1975; Fig. 5; Table 2). As a minor moraine system
448 partly controlled by topographic features, it is unlikely that correlations can be made with other
449 systems of the Québec-Labrador Dome. It probably represents subordinate recessional moraines
450 from the Sebaskachu Moraine located ~30 km to the east as suggested by the short time interval
451 (< 0.3 ka) separating both landforms.

452 To summarize, while the Brador, Belles Amours and Sebaskachu moraines are
453 particularly well-dated at ~12.9 ka, ~11.5 ka and ~8.4 ka respectively, the age of the Paradise
454 and Little Drunken moraines remains uncertain. In addition, published cosmogenic exposure
455 ages (Ullman et al., 2016) and recalibration of legacy radiocarbon ages (King, 1985) for the

456 deglaciation west of Lake Melville allow refining later positions of the LIS margin for the
457 interior of Québec-Labrador up to Churchill Falls and allow estimating the associated retreat
458 rates for that period. A radiocarbon age indicates that the ice margin was located at the head of
459 the Churchill River valley by 8.0 ka (King, 1985; Fig. 5; Table 2). Cosmogenic exposure ages
460 (Ullman et al., 2016) and radiocarbon ages (Blake, 1982; King, 1985) indicate that the ice
461 margin retreated rapidly to Lake Winokapau by ~7.6 ka and to Churchill Falls by ~7.5 ka (Fig. 5;
462 Table 2).

463 **Ice Sheet response to abrupt climatic forcings**

464 Controls on the formation of the Brador, Belles Amours and Sebaskachu moraines, which
465 yield robust ages (Fig. 4), are first investigated in this discussion. The significance of the
466 Paradise and Little Drunken moraines, less well dated, need further discussion as their timing
467 remain uncertain.

468 The occurrence of the Brador Moraine (12.9 ± 0.7 ka) roughly outlining the marine limit
469 (~140 m.a.s.l.) along the coast of easternmost Québec-Labrador was speculated as representing a
470 mass balance readjustment (re-equilibration) of the LIS when the calving ice margin reached the
471 Brador highlands following disconnection from the Newfoundland Ice Cap (Grant, 1992). The
472 role of the topography in stabilizing marine-based ice margins has been extensively discussed in
473 recent literature (e.g., Jamieson et al., 2012; Batchelor et al., 2019; Brouard and Lajeunesse,
474 2019). This role appears, however, to be secondary in this particular situation as the moraine is
475 also observed on the plateau between valleys. Although it is difficult to deny the role played by
476 the transition from marine- to land-based in stabilizing the ice margin, it probably reflects an
477 equilibrium state sufficient for stabilization following a readvance – evidenced by glaciotectonic

478 deformation – triggered by the sudden decrease in temperature by 2°C (Fig. 6; Rasmussen et al.,
479 2014) at the beginning of the YD (12.9 – 11.7 ka BP).

480 The age of the Belles Amours Moraine (11.5 ± 0.7 ka) suggests that it corresponds to the
481 Preboreal Oscillation (11.5 – 11.3 ka BP), which is outlined by a sharp fall in temperatures in
482 Greenland ice cores at the very beginning of the Holocene (Fig. 6; Kobashi et al., 2017).
483 Freshwater input into the North Atlantic by abrupt glacial lake drainages is postulated to have
484 provoked alteration of the AMOC that resulted in several prominent early Holocene abrupt
485 cooling events, including the Preboreal Oscillation, the 9.3 ka event and the 8.2 ka event (Barber
486 et al., 1999; Fisher et al., 2002; Alley and Ágústsdóttir, 2005; Fleitmann et al., 2008). These
487 freshwater inputs are expressed in the Labrador Sea as Detrital Carbonate Peaks (DCP)
488 associated with high concentration of ice-rafted debris (Jennings et al., 2015). In the case of the
489 Preboreal oscillation, it is considered to have been triggered by the drainage of the glacial Lake
490 Agassiz via the Mackenzie River (Fisher et al., 2002; Süfke et al., 2022) and corresponds in time
491 with DCP 1 (Fig. 6; Jennings et al., 2015).

492 The Sebaskachu (8.4 ± 0.6 ka) and Peter's (8.1 ± 0.7 ka) moraine ages closely correspond
493 to the well-known 8.2 ka cooling event recorded in various sediment cores in the North Atlantic
494 region (Barber et al., 1999; Kleiven et al., 2008; Jennings et al., 2015) and ice cores of the
495 Greenland Ice Sheet (Rasmussen et al., 2014). This cooling event is widely considered to be
496 caused by the drainage of glacial Lake Agassiz-Ojibway into the North Atlantic via the Hudson
497 Strait (e.g., Barber et al., 1999; Clark et al., 2004; Lajeunesse & St-Onge, 2008; Brouard et al.,
498 2021). Moraine crests in the Peter's vicinity are minor and may as well be topographically-
499 controlled, and hence climatically insignificant, recessional features. Nonetheless, the close
500 occurrence of both moraines has a clear temporal coincidence with the abrupt cooling event

501 related to the collapse of the LIS over the Hudson Bay at 8.2 ka and recorded in the Labrador Sea
502 as DCP 7 (Fig. 6; Jennings et al., 2015). However, the timing of the Sebaskachu Moraine at the
503 start of this event could also support the hypothesis of a broader cooling perturbation beginning
504 at ~8.6 ka BP (Rohling and Pälike, 2005; Morrill et al., 2013) as a response to the early opening
505 of the Tyrell Sea (Fig. 6; Jennings et al., 2015).

506 In view of the tightly clustered individual (n=5) ages for the Belles Amours Moraine
507 centered at 11.5 ± 0.3 ka, the ^{10}Be ages for the Paradise (12.1 ± 0.6 ka) and Little Drunken (10.6
508 ± 0.7 ka) moraines reported here are unlikely as they are unquestionably too old. Based on their
509 stratigraphic position, the Belles Amours Moraine is expected to be older in age than the
510 Paradise Moraine and, consequently, significantly older than the Little Drunken Moraine. To
511 cope with these discrepancies, published cosmogenic exposure ages (Ullman et al., 2016) were
512 incorporated in our age model. Their recalculations show ages of 9.4 ± 0.8 ka and 8.5 ± 0.7 ka
513 for the Paradise Moraine and Québec North Shore-Little Drunken Moraine, respectively (see
514 Supplementary Material; Table S3). While there are discrepancies between the ages from the
515 original publication and our recalculations, the uncertainties still overlap between datasets. Two
516 key parameters could however partly explain the younger ages of the samples in regard to the
517 actual targeted landforms: 1) Ullman et al. (2016) sampled boulders sometimes located well
518 behind morainic crests (up to 25 km), therefore systematically minimizing the moraine ages; and
519 2) some samples were collected below the reported marine limit of 150 m (Carlson, 2020) for the
520 site CL1, consequently delaying their exposure ages by a few centuries. These ages, representing
521 minimum values for the abandonment of the moraines, are nonetheless coherent with minimum-
522 limiting radiocarbon ages in the region and, consequently, complete our dataset without any
523 chronological overlap between moraine segments. Combining both datasets could therefore

524 allow the correlation of the Paradise Moraine to the 10.3 ka event and the Little Drunken
525 Moraine to the 9.3 ka event, as suggested by Ullman et al. (2016). While the cause of the 10.3 ka
526 cooling event remains elusive, its consequences, recorded by (1) the presence of DCP 2 (Fig. 6;
527 Jennings et al., 2015) and (2) the widespread stabilization of the ice margins in western
528 Greenland and eastern Canada (Young et al., 2020, 2021) are unequivocal and a correlation with
529 the major Paradise Moraine is most likely. The 9.3 ka event, which is correlated to DCP 3 or 4
530 (Fig. 6; Jennings et al., 2015), was speculated to have been triggered either by the Noble Inlet
531 readvance across Hudson Strait (Jennings et al., 2015) or a meltwater outburst flow from Lake
532 Superior (Yu et al., 2010). This abrupt cooling event has been recorded around Baffin Bay as a
533 widespread ice margin stabilization event (e.g., Lesnek et al., 2018; Crump et al., 2020; Young et
534 al., 2020) and may therefore correlate to the timing of deposition of the Little Drunken Moraine.
535 The occurrence of two stabilizations in Lake Melville (M1, M2 – Fig. 1C) could in fact
536 correspond to the two DCP peaks observed around that event, if the moraine system identified on
537 seismic data (M1) could be the result of a drawdown of the ice as speculated by several authors
538 (i.e., Fulton and Hodgson, 1979; Vilks et al., 1987). This drawdown into Lake Melville may have
539 provoked only a localized stabilization, although its occurrence elsewhere remains to be
540 determined.

541 Finally, the compilation of cosmogenic exposure ages presented here together with
542 previously published cosmogenic and radiocarbon ages allows identifying margin stabilizations
543 and/or readvances of the eastern fringe of the LIS at ~12.9, ~11.5, ~10.4, ~9.3 and ~8.4-8.2 ka.
544 This comprehensive ^{10}Be -based chronology clearly demonstrates that timing of moraine
545 deposition in easternmost Québec-Labrador was coeval with cold climatic events recorded in
546 Greenland ice cores (Fig. 6), indicating that the LIS margin was interconnected with climate

547 fluctuations at least regionally. The synchronicity of moraine deposition along the eastern fringe
548 of the LIS from Baffin Island to southern Québec – that connect both continental- and marine-
549 based segments of the ice margin – strongly suggests that readvances of the ice margin were
550 triggered by major, short-term regional climatic deteriorations rather than by a mechanical
551 adjustment or re-equilibration of the ice sheet (Hillaire-Marcel et al., 1981; Dubois and Dionne,
552 1985; Clark et al., 2000). This deglaciation chronology supports results from around Baffin Bay
553 suggesting that early Holocene ice margin readvances and/or stabilizations of the LIS – and
554 Greenland Ice Sheet – were caused by meltwater pulses into the Labrador Sea (Young et al.,
555 2020, 2021). Similar to their interpretation, detrital carbonate peaks from the Cartwright Saddle
556 on the Labrador Shelf (Jennings et al., 2015) preceding the stabilizations/readvances of the ice
557 margin in easternmost Québec-Labrador possibly indicate that abrupt cold reversals of the early
558 Holocene were strongly influenced by meltwater pulses weakening the AMOC. While early
559 Holocene cooling events appear to be triggered by freshwater input – often caused itself by
560 abrupt lake drainage – into the Atlantic Ocean and recorded by detrital carbonate events in the
561 Labrador Sea, further investigation should focus on identifying trigger mechanisms for such
562 freshwater outbursts. The 1000 to 1200-year cyclicity behind those cooling events may suggest
563 an external forcing that influence the rapid retreat of the ice margin prior to these events, thus
564 favouring meltwater outburst. First proposed by Denton and Karlén (1973) – and later advocated
565 by Bond et al. (1997) – the cyclicity of Holocene cooling events has been for decades very
566 puzzling to researchers. Bond-like events, speculated by some to be influenced by enhanced
567 solar activity (e.g., Bond et al., 2001), may certainly still be relevant to identify a source for such
568 cycles, although their occurrence may as well simply be the result of several trigger mechanisms
569 (Young et al., 2021).

570 **Retreat rates reflect long-term climatic trends**

571 Retreat rates across the study area likely reflect long-term (centennial- to millennial-
572 scale) climatic trends, with minimum recession during colder periods and increasing rates
573 corresponding to warming temperatures. Minimum recession rates of the LIS margin in
574 easternmost Québec-Labrador were observed during the YD ($\sim 25 \text{ m a}^{-1}$) and again between 9.3
575 and 8.2 ka ($\sim 50 \text{ m a}^{-1}$). The YD was marked by significant lower temperature over a relatively
576 long period of $\sim 1,200$ years (Fig. 6; Buizert et al., 2014), therefore contributing to a significant
577 slowdown in ice retreat. A similar assessment could be made for the period between 9.3 and 8.2
578 ka, when another significant reversal in the warming temperature trend is observed (Fig. 6;
579 Kobashi et al., 2017). Increasing retreat rates across the study area from 11.5 ka to 9.3 ka ($75\text{-}90$
580 m a^{-1}) could be linked to the warming climatic trend recorded in Greenland ice cores (Fig. 6;
581 Kobashi et al., 2017). Collapse of the LIS can be recorded after 8.2 ka – regardless of climatic
582 trend – as retreat rates started increasing drastically, reaching up to $1,000 \text{ m a}^{-1}$ by 7.5 ka (Fig. 6).

583 Several lines of explanation can be invoked to understand the collapse of the LIS in
584 central Québec-Labrador: 1) Rapidly increasing temperatures in the Arctic and subarctic regions
585 – similar as present-day observations – directly affecting its accumulation zone and resulting in
586 negative mass balance (Carlson et al., 2009); or 2) The Québec-Labrador Dome reached a
587 tipping point from which it was no longer in balance with climate and sustainable under early
588 Holocene climatic conditions. Recurrent climatic cooling phases provoked by meltwater
589 discharge events were suggested to have helped “artificially” sustain the Québec-Labrador Dome
590 during the early Holocene (Ullman et al., 2016). In this perspective, it is possible that the absence
591 of such events after 8.2 ka favored the collapse of the LIS as a lagged response to the overall
592 Holocene warming (Shakun et al., 2012; Buizert et al., 2018). With a constant negative mass-

593 balance at the time, the Québec-Labrador Dome eventually disappeared by 6 ka (Richard et al.,
594 1982; Clark et al., 2000; Jansson, 2003; Occhietti et al., 2011; Dubé-Loubert et al., 2018).

595 However, it can be stressed that calculating retreat rates between stabilizations of the ice
596 margin is only tentative in this situation, smoothing inappropriately the signal of ice sheet
597 readvances. Therefore, using an approach integrating estimates of hiatus duration (e.g., Lowell et
598 al., 2021) would be more appropriate in order to exclude uncertainties related to the length of
599 stabilizations and magnitude of potentially preceding readvances. This method would, however,
600 require further dating to better constrain the timing of the ice margin readvances and duration of
601 the stabilizations.

602 **Conclusion**

603 This paper reports on 37 new cosmogenic ^{10}Be and 4 new radiocarbon ages in
604 easternmost Québec-Labrador that allow establishing the chronological framework of major
605 moraine systems deposited during stabilizations/readvances stages of the LIS margin. These
606 results improve the deglaciation history drawn for the region by earlier workers and document
607 periods of regional ice margin stabilization at ~12.9, ~11.5, ~10.4, ~9.3 and ~8.4-8.2 ka. The
608 combined ages outline a close relationship between climate and glaciodynamics of the LIS
609 margin during the late Wisconsinan – early Holocene transition and is in line with previous work
610 on Baffin Island and western Greenland suggesting that glacial dynamics were controlled by
611 abrupt climatic events and possibly synchronous along the margin of entire ice sheets. The
612 physical connection between the easternmost Québec-Labrador moraines and other systems of
613 the eastern fringe of the LIS remains, however, ambiguous. Although correlations can be made
614 with major moraine systems of southern Québec, large geographical gaps and chronological
615 uncertainties persist. The transition between land- to marine-based ice margin makes it difficult

616 to accurately connect undated moraines from one region to another without a complete swath
617 bathymetric coverage offshore.

618 Future work focusing on connecting the easternmost Québec-Labrador moraine systems
619 with those of the Québec North Shore and northern Labrador is needed in order to provide a
620 larger-scale palaeogeographical perspective of the major stages of the LIS margin in a period of
621 rapid climatic fluctuations across a wide range of latitudes, as well as marine to continental
622 contexts. Further direct dating is needed on moraine systems across the Québec-Labrador region
623 to assess more precisely the extent of the LIS and the final stages of deglaciation at the YD-early
624 Holocene transition. A better chronological constraint would not only be essential for future
625 empirical-based numerical model assessing the contribution of the LIS to global sea-level
626 changes, but it would also greatly increase our understanding of abrupt climatic cooling events
627 induced by ice sheet-derived meltwater discharge into the North Atlantic. Although an almost
628 consistent cyclical pattern of ~1,000-1,200 years is observed between the major ice margin
629 stabilizations reported here during the early Holocene, the origin of these events as negative
630 feedback triggered by meltwater inputs into the North Atlantic has yet to be explored as an
631 analogue to potential forthcoming climate variation.

632 **Acknowledgments**

633 This project was funded by the ArcticNet Network of Centers of Excellence, Natural
634 Sciences and Engineering Council of Canada (NSERC) and Sentinelle Nord (Apogée Canada)
635 grants to P.L., Institut de Physique du Globe de Strasbourg (IPGS) grants to J.F.G, as well as
636 Université de Strasbourg and Fondation Famille Choquette grants to P.O.C. We are thankful to
637 the Centre d'études nordiques (CEN), Polar Knowledge Canada (POLAR) and SYSTER
638 research program from the CNRS-INSU for financial support during fieldwork. The French

639 national AMS facility ASTER (CEREGE) is supported by the INSU/CNRS, the French MESR,
640 and the CEA institute. We are thankful to G. Aumaître and K. Keddadouche for the AMS
641 measurements. We thank Charles Brionne, Etienne Brouard and Vincent Rinterknecht who
642 provided helpful comments on a previous draft of the paper.

643 **References**

- 644 Alley, R. B., Mayewski, P. A., Sowers, T., Stuiver, M., Taylor, K. C., Clark, P. U., 1997.
645 Holocene climatic instability: A prominent, widespread event 8200 yr ago. *Geology* 25(6),
646 483-486.
- 647 Alley, R. B., Ágústsdóttir, A. M., 2005. The 8 ka event: cause and consequences of a major
648 Holocene abrupt climate change. *Quaternary Science Reviews* 24(10-11), 1123-1149.
- 649 Andrews, J. T., 1963. End moraines and late-glacial chronology in the northern Nain-Okak
650 section of the Labrador coast. *Geografiska Annaler* 45(2-3), 158-171.
- 651 Andrews, J. T., Falconer, G., 1969. Late glacial and post-glacial history and emergence of the
652 Ottawa Islands, Hudson Bay, Northwest Territories: Evidence on the deglaciation of
653 Hudson Bay. *Canadian Journal of Earth Sciences* 6(5), 1263-1276.
- 654 Andrews, J. T., Ives, J. D., 1978. "Cockburn" Nomenclature and the Late Quaternary History of
655 the Eastern Canadian Arctic. *Arctic and Alpine Research* 10(3), 617-633.
- 656 Awadallah, S. A., Batterson, M. J., 1990. Comment on "late deglaciation of the central Labrador
657 coast and its implications for the age of glacial lakes Naskaupi and McLean and for
658 prehistory," by Clark, P. U., and Fitzhugh W. W., *Quaternary Research* 34(3), 372-373.
- 659 Axford, Y., Briner, J. P., Miller, G. H., Francis, D. R., 2009. Paleoecological evidence for abrupt
660 cold reversals during peak Holocene warmth on Baffin Island, Arctic Canada. *Quaternary
661 Research* 71(2), 142-149.
- 662 Balco, G., Stone, J. O., Lifton, N. A., Dunai, T. J., 2008. A complete and easily accessible means
663 of calculating surface exposure ages or erosion rates from ¹⁰Be and ²⁶Al measurements.
664 *Quaternary Geochronology* 3(3), 174-195.
- 665 Balco, G., Briner, J., Finkel, R. C., Rayburn, J. A., Ridge, J. C., Schaefer, J. M., 2009. Regional
666 beryllium-10 production rate calibration for late-glacial northeastern North America.
667 *Quaternary Geochronology* 4(2), 93-107.
- 668 Balco, G., 2020. Glacier change and paleoclimate applications of cosmogenic-nuclide exposure
669 dating. *Annual Review of Earth and Planetary Sciences* 48, 21-48.
- 670 Barber, D. C., Dyke, A., Hillaire-Marcel, C., Jennings, A. E., Andrews, J. T., Kerwin, M. W.,
671 Bilodeau, G., McNeely, R., Southon, J., Morehead, M. D., Gagnon, J. M., 1999. Forcing of
672 the cold event of 8,200 years ago by catastrophic drainage of Laurentide lakes. *Nature*
673 400(6742), 344-348.
- 674 Batchelor, C. L., Dowdeswell, J. A., Rignot, E., Millan, R., 2019. Submarine moraines in
675 Southeast Greenland fjords reveal contrasting outlet- glacier behaviour since the Last
676 Glacial Maximum. *Geophysical Research Letters* 46, 3279–3286.
- 677 Bierman, P. R., Caffee, M. W., Davis, P. T., Marsella, K., Pavich, M., Colgan, P., Mickelson, D.,
678 Larsen, J., 2002. Rates and timing of earth surface processes from in situ-produced
679 cosmogenic Be-10. *Reviews in Mineralogy and Geochemistry* 50 (1), 147-205.
- 680 Blake, W. Jr., 1956. Landforms and topography of the Lake Melville area, Labrador,

681 Newfoundland. Canada Department of Mines and Technical Surveys Geographical Bulletin
682 9, 93–97.

683 Bond, G., Showers, W., Cheseby, M., Lotti, R., Almasi, P., DeMenocal, P., Priore, P., Cullen,
684 H., Hajdas, I., Bonani, G., 1997. A pervasive millennial-scale cycle in North Atlantic
685 Holocene and glacial climates. *Science* 278(5341), 1257-1266.

686 Bond, G., Kromer, B., Beer, J., Muscheler, R., Evans, M. N., Showers, W., Hoffman, S., Lotti-
687 Bond, R., Hajdas, I., Bonani, G., 2001. Persistent solar influence on North Atlantic climate
688 during the Holocene. *Science* 294(5549), 2130-2136.

689 Borchers, B., Marrero, S., Balco, G., Caffee, M., Goehring, B., Lifton, N., Nishiizumi, K.,
690 Phillips, P., Schaefer, J. Stone, J., 2016. Geological calibration of spallation production
691 rates in the CRONUS-Earth project. *Quaternary Geochronology* 31, 188-198.

692 Braucher, R., Guillou, V., Bourlès, D. L., Arnold, M., Aumaître, G., Keddadouche, K., Nottoli,
693 E., 2015. Preparation of ASTER in-house $^{10}\text{Be}/^{9}\text{Be}$ standard solutions. *Nuclear*
694 *Instruments and Methods in Physics Research Section B: Beam Interactions with Materials*
695 *and Atoms* 361, 335-340.

696 Briner, J. P., Miller, G. H., Davis, P. T., Finkel, R. C., 2005. Cosmogenic exposure dating in
697 arctic glacial landscapes: implications for the glacial history of northeastern Baffin Island,
698 Arctic Canada. *Canadian Journal of Earth Sciences* 42(1), 67-84.

699 Briner, J. P., Overeem, I., Miller, G., Finkel, R., 2007. The deglaciation of Clyde Inlet,
700 northeastern Baffin Island, Arctic Canada. *Journal of Quaternary Science* 22(3), 223-232.

701 Briner, J. P., Bini, A. C., Anderson, R. S., 2009. Rapid early Holocene retreat of a Laurentide
702 outlet glacier through an Arctic fjord. *Nature Geoscience* 2(7), 496-499.

703 Briner, J. P., Cuzzone, J. K., Badgley, J. A., Young, N. E., Steig, E. J., Morlighem, M.,
704 Schlegel, N.-J., Hakim, G. J., Schaefer, J. M., Johnson, J. V., Lesnek, A. J., Thomas, E. K.,
705 Allan, E., Bennike, O., Cluett, A. A., Csatho, B., de Vernal, A., Downs, J., Larour, E.,
706 Nowicki, S., 2020. Rate of mass loss from the Greenland Ice Sheet will exceed Holocene
707 values this century. *Nature* 586(7827), 70-74.

708 Bromley, G. R., Hall, B. L., Thompson, W. B., Kaplan, M. R., Garcia, J. L., Schaefer, J. M.,
709 2015. Late glacial fluctuations of the Laurentide ice sheet in the White Mountains of Maine
710 and New Hampshire, USA. *Quaternary Research* 83(3), 522-530.

711 Brouard, E., Lajeunesse, P., 2019. Glacial to postglacial submarine landform assemblages in
712 fjords of northeastern Baffin Island. *Geomorphology* 330, 40-56.

713 Brouard, E., Roy, M., Godbout, P. M., Veillette, J. J., 2021. A framework for the timing of the
714 final meltwater outbursts from glacial Lake Agassiz-Ojibway. *Quaternary Science Reviews*
715 274, 107269.

716 Bryson, R. A., Wendland, W. M., Ives, J. D., Andrews, J. T., 1969. Radiocarbon isochrones on
717 the disintegration of the Laurentide Ice Sheet. *Arctic and Alpine Research* 1(1), 1-13.

718 Buizert, C., Gkinis, V., Severinghaus, J. P., He, F., Lecavalier, B. S., Kindler, P., Leuenberger,
719 M., Carlson, A. E., Vinther, B., Masson-Delmotte, V., White, J. W. C., Liu, Z., Otto-

- 720 Bliesner, B., Brook, E. J., 2014. Greenland temperature response to climate forcing during
721 the last deglaciation. *Science* 345(6201), 1177-1180.
- 722 Carlson, A. E., LeGrande, A. N., Oppo, D. W., Came, R. E., Schmidt, G. A., Anslow, F. S.,
723 Licciardi, J. M., Obbink, E. A., 2008. Rapid early Holocene deglaciation of the Laurentide
724 ice sheet. *Nature Geoscience* 1(9), 620-624.
- 725 Carlson, A. E., Clark, P. U., Haley, B. A., Klinkhammer, G. P., 2009. Routing of western
726 Canadian Plains runoff during the 8.2 ka cold event. *Geophysical Research Letters* 36(14).
- 727 Carlson, A. E., Clark, P. U., 2012. Ice sheet sources of sea level rise and freshwater discharge
728 during the last deglaciation. *Reviews of Geophysics* 50(4), RG4007.
- 729 Carlson, A. E., 2020. Comment on: Deglaciation of the Greenland and Laurentide ice sheets
730 interrupted by glacier advance during abrupt coolings. *Quaternary Science Reviews* 240,
731 106354.
- 732 Chmeleff, J., von Blanckenburg, F., Kossert, K., Jakob, D., 2010. Determination of the ^{10}Be
733 half-life by multicollector ICP-MS and liquid scintillation counting. *Nuclear Instruments*
734 *and Methods in Physics Research Section B: Beam Interactions with Materials and Atoms*
735 268(2), 192-199.
- 736 Clark, C. D., Knight, J. K., Gray, J. T., 2000. Geomorphological reconstruction of the Labrador
737 sector of the Laurentide Ice Sheet. *Quaternary Science Reviews* 19(13), 1343-1366.
- 738 Clark, P. U., Fitzhugh, W. W., 1990. Late deglaciation of the central Labrador coast and its
739 implications for the age of glacial lakes Naskaupi and McLean and for prehistory.
740 *Quaternary Research* 34(3), 296-305.
- 741 Clark, P. U., Brook, E. J., Raisbeck, G. M., Yiou, F., Clark, J., 2003. Cosmogenic ^{10}Be ages of
742 the Saglek Moraines, Torngat Mountains, Labrador. *Geology* 31(7), 617-620.
- 743 Coleman, A. P., 1921. Northwestern part of Labrador and New Quebec. Canada, Geological
744 Survey, Memoir 124.
- 745 Crump, S. E., Young, N. E., Miller, G. H., Pendleton, S. L., Tulenko, J. P., Anderson, R. S.,
746 Briner, J. P., 2020. Glacier expansion on Baffin Island during early Holocene cold reversals.
747 *Quaternary Science Reviews* 241, 106419.
- 748 Dalton, A.S., Margold, M., Stokes, C.R., Tarasov, L., Dyke, A.S., Adams, R.S., Allard, S.,
749 Arends, H.E., Atkinson, N., Attig, J.W., Barnett, P.J., Barnett, R.L., Batterson, M.,
750 Bernatchez, P., Borns, H.W., Breckenridge, A., Briner, J.P., Brouard, E., Campbell, J.E.,
751 Carlson, A.E., Clague, J.J., Curry, B.B., Daigneault, R.A., Dubé-Loubert, H., Easterbrook,
752 D.J., Franzi, D.A., Friedrich, H.G., Funder, S., Gauthier, M.S., Gowan, A.S., Harris, K.L.,
753 Héту, B., Hooyer, T.S., Jennings, C.E., Johnson, M.D., Kehew, A.E., Kelley, S.E., Kerr, D.,
754 King, E.L., Kjeldsen, K.K., Knaeble, A.R., Lajeunesse, P., Lakeman, T.R., Lamothe, M.,
755 Larson, P., Lavoie, M., Loope, H.M., Lowell, T.V., Lusardi, B.A., Manz, L., McMartin, I.,
756 Nixon, F.C., Occhietti, S., Parkhill, M.A., Piper, D.J.W., Pronk, A.G., Richard, P.J.H.,
757 Ridge, J.C., Ross, M., Roy, M., Seaman, A., Shaw, J., Stea, R.R., Teller, J.T., Thompson,
758 W.B., Thorleifson, L.H., Utting, D.J., Veillette, J.J., Ward, B.C., Weddle, T.K., Wright,
759 H.E., 2020. An updated radiocarbon-based ice margin chronology for the last deglaciation

- 760 of the North American Ice Sheet Complex. *Quaternary Science Reviews* 234, 106223.
- 761 Davis, P. T., Bierman, P. R., Corbett, L. B. Finkel, R. C., 2015. Cosmogenic exposure age
762 evidence for rapid Laurentide deglaciation of the Katahdin area, west-central Maine, USA,
763 16 to 15 ka. *Quaternary Science Reviews*, 116, 95-105.
- 764 Denton, G. H., Karlén, W., 1973. Holocene climatic variations—their pattern and possible cause.
765 *Quaternary Research* 3(2), 155-205.
- 766 Denton, G. H., Anderson, R. F., Toggweiler, J. R., Edwards, R. L., Schaefer, J. M., Putnam, A.
767 E., 2010. The last glacial termination. *Science* 328(5986), 1652-1656.
- 768 Dietrich, P., Ghienne, J. F., Normandeau, A., Lajeunesse, P., 2017. Reconstructing ice-margin
769 retreat using delta morphostratigraphy. *Scientific Reports* 7(1), 16936.
- 770 Dietrich, P., Ghienne, J. F., Lajeunesse, P., Normandeau, A., Deschamps, R., Razin, P., 2019.
771 Deglacial sequences and glacio-isostatic adjustment: Quaternary compared with Ordovician
772 glaciations. Geological Society, London, Special Publications 475(1), 149-179.
- 773 Dietrich, P., Normandeau, A., Lajeunesse, P., Ghienne, J. F., Schuster, M., Nutz, A., 2020.
774 Deltaic Complexes of the Québec North Shore. In Slaymaker, O., Catto, N. (Eds),
775 Landscapes and Landforms of Eastern Canada. Springer, Cham, 245-258.
- 776 Dubé-Loubert, H., Roy, M., Schaefer, J. M., Clark, P. U., 2018. 10Be dating of former glacial
777 Lake Naskaupi (Québec-Labrador) and timing of its discharges during the last deglaciation.
778 *Quaternary Science Reviews* 191, 31-40.
- 779 Dubois, J. M., Dionne, J. C., 1985. The Québec North Shore moraine system: A major feature of
780 Late Wisconsin déglaciation. *Geological Society of America Special Papers* 197, 125-134.
- 781 Dyke, A. S., 1979. Glacial and sea-level history of southwestern Cumberland Peninsula, Baffin
782 Island, NWT, Canada. *Arctic and Alpine Research* 11(2), 179-202.
- 783 Dyke, A. S., Prest, V. K., 1987. Late Wisconsinan and Holocene History of the Laurentide Ice
784 Sheet. *Géographie physique et Quaternaire* 41, 237-263.
- 785 Dyke, A.S., Moore, A., Robertson, L., 2003. Deglaciation of North America: Thirty-two digital
786 maps at 1:7 000 000 scale with accompanying digital chronological database and one poster
787 (two sheets) with full map series. Geological Survey Canada Open File 1574.
- 788 Dyke, A. S., 2004. An outline of North American deglaciation with emphasis on central and
789 northern Canada. *Developments in Quaternary Sciences* 2, 373-424.
- 790 Engstrom, D. R., Hansen, B. C. S., 1985. Postglacial vegetational change and soil development
791 in southeastern Labrador as inferred from pollen and chemical stratigraphy. *Canadian*
792 *Journal of Botany* 63(3), 543-561.
- 793 Fisher, T. G., Smith, D. G., Andrews, J. T., 2002. Preboreal oscillation caused by a glacial Lake
794 Agassiz flood. *Quaternary Science Reviews* 21(8-9), 873-878.
- 795 Fleitmann, D., Mudelsee, M., Burns, S. J., Bradley, R. S., Kramers, J., Matter, A., 2008.
796 Evidence for a widespread climatic anomaly at around 9.2 ka before present.
797 *Paleoceanography* 23(1), PA1102.

- 798 Fulton, R.J., Hodgson, D.A., 1979. Wisconsin glacial retreat, Southern Labrador. Current
799 Research, Part C, Geological Survey of Canada, Paper 79-1C, 17–21.
- 800 Gebardht, C., Ohlendorf, C., Gross, F., Matthiessen, J., Schneider, R., 2020. Development of the
801 Labrador Shelf During the Past Glaciations, Cruise No. MSM84, June 19 to July 16, 2019,
802 St. Johns (Canada) - St. Johns (Canada). Maria S. Merian Berichte, Gutachterpanel
803 Forschungsschiffe, Bonn, 78 pp.
- 804 Grant, D. R., 1992. Quaternary Geology of St. Anthony-Blanc-Sablon Area, Newfoundland and
805 Quebec. Geological Survey of Canada. 69 pp.
- 806 Greene, B. A., 1974. An outline of the geology of Labrador. *Geoscience Canada* 1(3), 36-40.
- 807 Hardy, L., 1982. La moraine frontale de Sakami, Québec subarctique. *Géographie physique et*
808 *Quaternaire* 36(1-2), 51-61.
- 809 Harington, C., Anderson, T., Rodrigues, C., 1993. Pleistocene walrus (*Odobenus rosmarus*) from
810 Forteau, Labrador. *Géographie physique et Quaternaire* 47(1), 111-118.
- 811 He, F., Clark, P. U., 2022. Freshwater forcing of the atlantic meridional overturning circulation
812 revisited. *Nature Climate Change* 12(5), 449-454.
- 813 Hillaire-Marcel, C., Occhietti, S., Vincent, J. S., 1981. Sakami moraine, Quebec: a 500-km-long
814 moraine without climatic control. *Geology* 9(5), 210-214.
- 815 Hodgson, D. A., Fulton, R. J., 1972. Site description, age and significance of a shell sample from
816 the mouth of the Michael River, 30 km south of Cape Harrison, Labrador. Report of
817 Activities, Part B, Geological Survey of Canada, Paper 72-1, 102-105.
- 818 Hynes, A., Rivers, T., 2010. Protracted continental collision—Evidence from the Grenville
819 orogen. *Canadian Journal of Earth Sciences* 47(5), 591-620.
- 820 Ives, J. D., 1978. The maximum extent of the Laurentide Ice Sheet along the east coast of North
821 America during the last glaciation. *Arctic*, 24-53.
- 822 Jamieson, S. S., Vieli, A., Livingstone, S. J., Cofaigh, C. Ó., Stokes, C., Hillenbrand, C. D.,
823 Dowdeswell, J. A., 2012. Ice-stream stability on a reverse bed slope. *Nature Geoscience*
824 5(11), 799-802.
- 825 Jansson, K. N., 2003. Early Holocene glacial lakes and ice marginal retreat pattern in
826 Labrador/Ungava, Canada. *Palaeogeography, Palaeoclimatology, Palaeoecology* 193(3-4),
827 473-501.
- 828 Jennings, A., Andrews, J., Pearce, C., Wilson, L., Ólfasdóttir, S., 2015. Detrital carbonate peaks
829 on the Labrador shelf, a 13–7 ka template for freshwater forcing from the Hudson Strait
830 outlet of the Laurentide Ice Sheet into the subpolar gyre. *Quaternary Science Reviews* 107,
831 62-80.
- 832 Josenhans, H.W., Zevenhuizen, J., Klassen, R.A., 1986. The Quaternary geology of the Labrador
833 Shelf. *Canadian Journal of Earth Sciences* 23, 1190–1213.
- 834 King, G., 1985. A standard method for evaluating radiocarbon dates of local deglaciation:
835 application to the deglaciation history of southern Labrador and adjacent Québec.

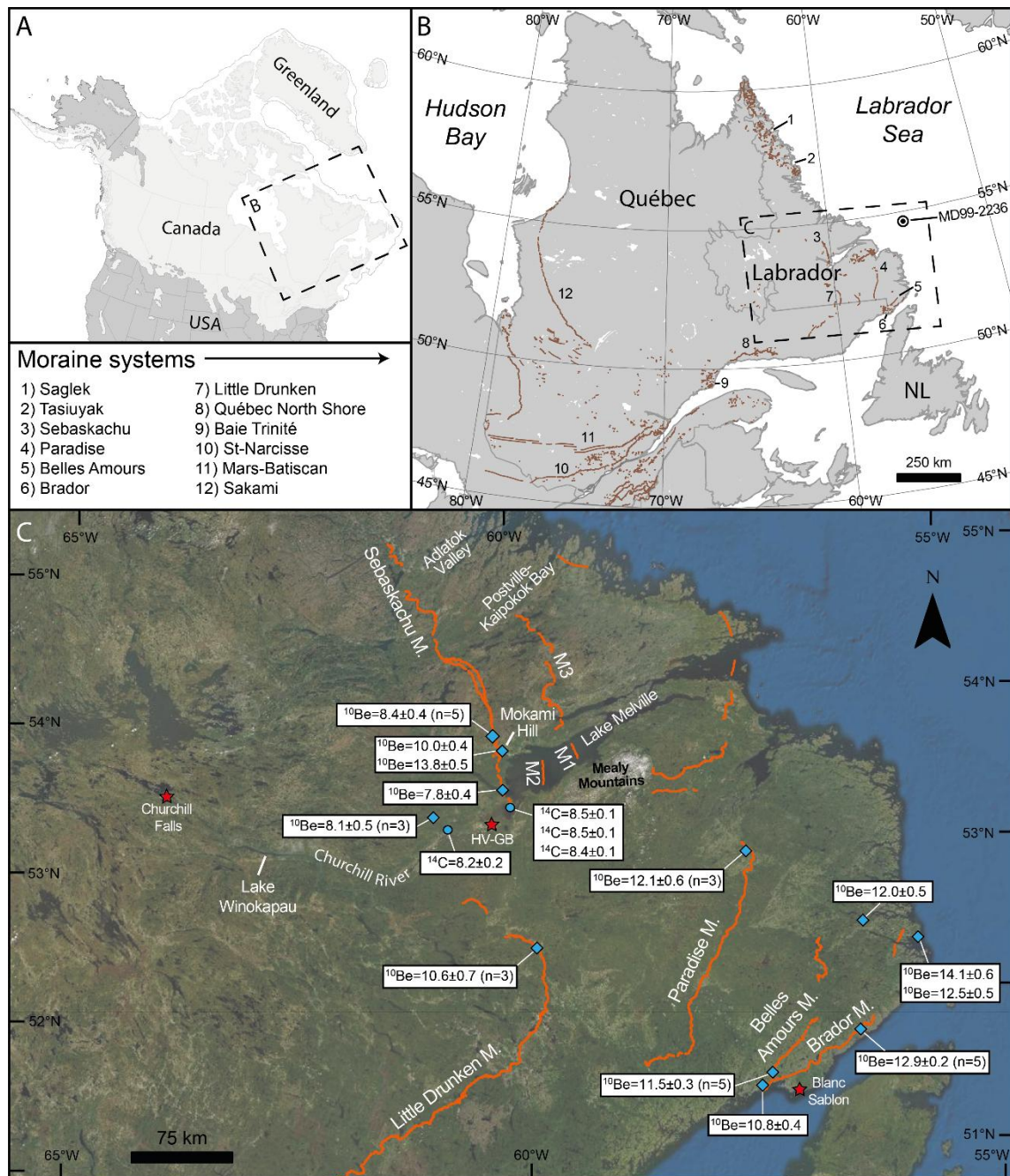
- 836 Géographie physique et Quaternaire 39(2), 163-182.
- 837 Klassen, R.A., Paradis, S., Bolduc, A.M., Thomas, R.D., 1992. Glacial landforms and deposits,
838 Labrador, Newfoundland and eastern Québec. Geological Survey of Canada, Map 1814A,
839 scale 1:1 000 000.
- 840 Kleiven, H. K. F., Kissel, C., Laj, C., Ninnemann, U. S., Richter, T. O., Cortijo, E., 2008.
841 Reduced North Atlantic deep water coeval with the glacial Lake Agassiz freshwater
842 outburst. *Science* 319(5859), 60-64.
- 843 Kobashi, T., Menviel, L., Jeltsch-Thömmes, A., Vinther, B. M., Box, J. E., Muscheler, R.,
844 Nakaegawa, T., Pfister, P. L., Döring, M., Leuenberger, M., Wanner, H., Ohmura, A., 2017.
845 Volcanic influence on centennial to millennial Holocene Greenland temperature change.
846 *Scientific reports* 7(1), 1-10.
- 847 Kohl, C.P., Nishiizumi, K., 1992. Chemical isolation of quartz for measurement of in-situ-
848 produced cosmogenic nuclides. *Geochimica et Cosmochimica Acta* 56, 3583-3587.
- 849 Korschinek, G., Bergmaier, A., Faestermann, T., Gerstmann, U. C., Knie, K., Rugel, G.,
850 Wallner, A., Dillmann, I., Dollinger, G., Lierse von Gostomski, C., Kossert, K., Maiti, M.,
851 Poutivtsev, M., Remmert, A., 2010. A new value for the half-life of ^{10}Be by heavy-ion
852 elastic recoil detection and liquid scintillation counting. *Nuclear Instruments and Methods*
853 *in Physics Research Section B: Beam Interactions with Materials and Atoms* 268(2), 187-
854 191.
- 855 Lajeunesse, P., Allard, M., 2003. The Nastapoka drift belt, eastern Hudson Bay: implications of a
856 stillstand of the Quebec Labrador ice margin in the Tyrrell Sea at 8 ka BP. *Canadian Journal*
857 *of Earth Sciences* 40(1), 65-76.
- 858 Lajeunesse, P., St-Onge, G., 2008. The subglacial origin of the Lake Agassiz–Ojibway final
859 outburst flood. *Nature Geoscience* 1(3), 184-188.
- 860 Lajeunesse, P., Dietrich, P., Ghienne, J. F., 2019. Late Wisconsinan grounding zones of the
861 Laurentide Ice Sheet margin off the Québec North Shore (NW Gulf of St Lawrence).
862 Geological Society, London, Special Publications 475(1), 241-259.
- 863 Lal, D., 1991, Cosmic ray labeling of erosion surfaces: in situ nuclide production rates and
864 erosion models. *Earth and Planetary Science Letters* 104, 424-439.
- 865 Lamb, H. F., 1978. Post-glacial Vegetation Change in Southeastern Labrador, M. Sc. thesis.
866 University of Minnesota, Minneapolis, Minnesota, 101 p.
- 867 Lamb, H. F., 1980. Late Quaternary vegetational history of southeastern Labrador. *Arctic and*
868 *Alpine Research* 12(2), 117-135.
- 869 Lamb, H. F., 1985. Palynological evidence for postglacial change in the position of tree limit in
870 Labrador. *Ecological Monographs* 55(2), 241-258.
- 871 Lesnek, A. J., Briner, J. P., 2018. Response of a land-terminating sector of the western Greenland
872 Ice Sheet to early Holocene climate change: Evidence from ^{10}Be dating in the Søndre
873 Isortoq region. *Quaternary Science Reviews* 180, 145-156.

- 874 Lesnek, A. J., Briner, J. P., Young, N. E., Cuzzone, J. K., 2020. Maximum southwest Greenland
875 Ice Sheet recession in the early Holocene. *Geophysical Research Letters* 47(1),
876 e2019GL083164.
- 877 Leydet, D. J., Carlson, A. E., Teller, J. T., Breckenridge, A., Barth, A. M., Ullman, D. J.,
878 Sinclair, G., Milne, G. A., Cuzzone, J. K., Caffee, M. W., 2018. Opening of glacial Lake
879 Agassiz's eastern outlets by the start of the Younger Dryas cold period. *Geology* 46(2), 155-
880 158.
- 881 Lifton, N., Sato, T., Dunai, T.J., 2014. Scaling in situ cosmogenic nuclide production rates using
882 analytical approximations to atmospheric cosmic-ray fluxes. *Earth Planetary Science Letters*
883 386, 149-160.
- 884 Long, A. J., Woodroffe, S. A., Dawson, S., Roberts, D. H., Bryant, C. L., 2009. Late Holocene
885 relative sea level rise and the Neoglacial history of the Greenland ice sheet. *Journal of*
886 *Quaternary Science* 24(4), 345-359.
- 887 Lowdon, J. A., Blake, W. Jr., 1973. Geological Survey of Canada radiocarbon dates XIII,
888 Geological Survey of Canada, Paper 73-7, 61 p.
- 889 Lowdon, J. A., Blake, W. Jr., 1975. Geological Survey of Canada radiocarbon dates XV,
890 Geological Survey of Canada, Paper 75-7, 32 p.
- 891 Lowdon, J. A., Blake, W. Jr., 1979. Geological Survey of Canada radiocarbon dates XIX;
892 Geological Survey of Canada, Paper 79-7, 58 p.
- 893 Lowdon, J. A., Blake, W. Jr., 1980. Geological Survey of Canada radiocarbon dates XX,
894 Geological Survey of Canada, Paper 80-7, 28 p.
- 895 Lowell, T. V., Kelly, M. A., Howley, J. A., Fisher, T. G., Barnett, P. J., Schwartz, R.,
896 Zimmerman, S. R. H., Norris, N., Malone, A. G., 2021. Near-constant retreat rate of a
897 terrestrial margin of the Laurentide Ice Sheet during the last deglaciation. *Geology* 49(12),
898 1511-1515.
- 899 Margreth, A., Gosse, J. C., Dyke, A. S., 2017. Wisconsinan and early Holocene glacial dynamics
900 of Cumberland peninsula, Baffin Island, arctic Canada. *Quaternary Science Reviews* 168,
901 79-100.
- 902 Marsella, K. A., Bierman, P. R., Davis, P. T., Caffee, M. W., 2000. Cosmogenic ^{10}Be and ^{26}Al
903 ages for the last glacial maximum, eastern Baffin Island, Arctic Canada. *Geological Society*
904 *of America Bulletin* 112(8), 1296-1312.
- 905 McManus, J. F., Francois, R., Gherardi, J. M., Keigwin, L. D., Brown-Leger, S., 2004. Collapse
906 and rapid resumption of Atlantic meridional circulation linked to deglacial climate changes.
907 *Nature* 428(6985), 834-837.
- 908 McNeely, R., Dyke, A. S., Southon, J. R., 2006. Canadian marine reservoir ages, preliminary
909 data assessment. Geological Survey of Canada, Open File 5049.
- 910 Miller, G. H., 1980. Late foxe glaciation of southern Baffin Island, NWT, Canada. *Geological*
911 *Society of America Bulletin* 91(7), 399-405.

- 912 Morrill, C., Anderson, D. M., Bauer, B. A., Buckner, R., Gille, E. P., Gross, W. S., Hartman, M.,
913 Shah, A., 2013. Proxy benchmarks for intercomparison of 8.2 ka simulations. *Climate of the*
914 *Past* 9(1), 423-432.
- 915 Morrison, A., 1970. Pollen diagrams from interior Labrador. *Canadian Journal of Botany* 48(11),
916 1957-1975.
- 917 Occhietti, S., 2007. The Saint-Narcisse morainic complex and early Younger Dryas events on the
918 southeastern margin of the Laurentide Ice Sheet. *Géographie physique et Quaternaire* 61(2-
919 3), 89-117.
- 920 Occhietti, S., Parent, M., Lajeunesse, P., Robert, F., Govare, E., 2011. Late Pleistocene–Early
921 Holocene decay of the Laurentide Ice Sheet in Québec–Labrador. *Developments in*
922 *Quaternary Science* 15, 601-630.
- 923 Piper, D. J., 1991. Seabed geology of the Canadian eastern continental shelf. *Continental Shelf*
924 *Research* 11(8-10), 1013-1035.
- 925 Putnam, A. E., Bromley, G. R., Rademaker, K., Schaefer, J. M., 2019. In situ ^{10}Be production-
926 rate calibration from a ^{14}C -dated late-glacial moraine belt in Rannoch Moor, central
927 Scottish Highlands. *Quaternary Geochronology* 50, 109-125.
- 928 Rasmussen, S. O., Bigler, M., Blockley, S. P., Blunier, T., Buchardt, S. L., Clausen, H. B.,
929 Cvijanovic, I., Dahl-Jensen, D., Johnson, S. J., Fischer, H., Gkinis, V., Guillevic, M., Hoek,
930 W.Z., John Lowe, J., Pedro, J. B., Popp, T., Seierstad, I. K., Steffensen, J. P., Svendsen, A.
931 M., Vallelonga, P., Vinther, B. M., Walker, M. J. C., Wheatley, J. J., Winstrup, M., 2014. A
932 stratigraphic framework for abrupt climatic changes during the Last Glacial period based on
933 three synchronized Greenland ice-core records: refining and extending the INTIMATE
934 event stratigraphy. *Quaternary Science Reviews* 106, 14-28.
- 935 Recq, C., Bhiry, N., Todisco, D., Buisson, E., Lauer, T., Rinterknecht, V. R., 2020. Local records
936 of former ice-sheet margins: geomorphological dynamics and sea-level evolution in the
937 Nain archipelago (Labrador, Atlantic Canada). In *GSA 2020 Connects Online*.
- 938 Reimer, P. J., Austin, W. E. N., Bard, E., Bayliss, A., Blackwell, P. G., Bronk Ramsey, C.,
939 Butzin, M., Cheng, H., Edwards, R. L., Friedrich, M., Grootes, P. M., Guilderson, T.P.,
940 Hajdas, I., Heaton, T. J., Hogg, A. G., Hughen, K. A., Kromer, B., Manning, S. W.,
941 Muscheler, R., Palmer, J. G., Pearson, C., Plicht, J. Van Der, Reimer, R. W., Richards, D.
942 A., Scott, E. M., Southon, J. R., Turney, C. S. M., Wacker, L., Adolphi, F., Büntgen, U.,
943 Capano, M., Fahrni, S. M., Fogtmann-Schulz, A., Friedrich, R., Köhler, P., Kudsk, S.,
944 Miyake, F., Olsen, J., Reinig, F., Sakamoto, M., Sookdeo, A., Talamo, S., 2020. The
945 IntCal20 northern Hemisphere radiocarbon age calibration curve (0-55 cal kBP).
946 *Radiocarbon*, 62(4), 725-757.
- 947 Richard, P. J. H., Larouche, A., Bouchard, M. A., 1982. Âge de la déglaciation finale et histoire
948 postglaciaire de la végétation dans la partie centrale du Nouveau-Québec. *Géographie*
949 *Physique et Quaternaire* 36, 63–90.
- 950 Roger, J., Saint-Ange, F., Lajeunesse, P., Duchesne, M. J., St-Onge, G., 2013. Late Quaternary
951 glacial history and meltwater discharges along the Northeastern Newfoundland Shelf.
952 *Canadian Journal of Earth Sciences* 50(12), 1178-1194.

- 953 Rohling, E. J., Pälike, H., 2005. Centennial-scale climate cooling with a sudden cold event
954 around 8,200 years ago. *Nature* 434(7036), 975-979.
- 955 Shaw, J., Piper, D. J. W., Fader, G. B. J., King, E. L., Todd, B. J., Bell, T., Batterson, M. J.,
956 Liverman, D. G. E., 2006. A conceptual model of the deglaciation of Atlantic Canada.
957 *Quaternary Science Reviews* 25(17-18), 2059-2081.
- 958 Stone, J.O., 2000. Air pressure and cosmogenic isotope production. *Journal of Geophysical*
959 *Research* 105 (23),753 23,759.
- 960 Stuiver, M., Reimer, P. J., 1993. Extended ¹⁴C database and revised CALIB radiocarbon
961 calibration program. *Radiocarbon* 35, 215-230.
- 962 Sufke, F., Gutjahr, M., Keigwin, L. D., Reilly, B., Giosan, L., Lippold, J., 2022. Arctic drainage
963 of Laurentide Ice Sheet meltwater throughout the past 14,700 years. *Communications Earth*
964 *& Environment* 3(1), 1-11.
- 965 Syvitski, J. P., Lee, H. J., 1997. Postglacial sequence stratigraphy of Lake Melville, Labrador.
966 *Marine Geology* 143(1-4), 55-79.
- 967 Ullman, D. J., Carlson, A. E., Hostetler, S. W., Clark, P. U., Cuzzone, J., Milne, G. A., Winsor,
968 K., Caffee, M. 2016. Final Laurentide ice-sheet deglaciation and Holocene climate-sea level
969 change. *Quaternary Science Reviews* 152, 49-59.
- 970 Vilks, G., Mudie, P. J., 1978. Early deglaciation of the Labrador Shelf. *Science* 202(4373), 1181-
971 1183.
- 972 Vilks, G., Hardy, I. A., Josenhans, H. W., 1984. Late Quaternary stratigraphy of the inner
973 Labrador Shelf. *Current Research, part A. Geological Survey of Canada, Paper 84-1A*, 57-
974 65.
- 975 Vilks, G., Deonarine, B., Winters, G., 1987. Late Quaternary marine geology of Lake Melville,
976 Labrador. *Geological Survey of Canada, Paper 87-22*, 50 p.
- 977 Young, N. E., Briner, J. P., Rood, D. H., Finkel, R. C., 2012. Glacier extent during the Younger
978 Dryas and 8.2-ka event on Baffin Island, Arctic Canada. *Science* 337(6100), 1330-1333.
- 979 Young, N. E., Schaefer, J. M., Briner, J. P., Goehring, B. M., 2013. A ¹⁰Be production- rate
980 calibration for the Arctic. *Journal of Quaternary Science* 28(5), 515-526.
- 981 Young, N. E., Briner, J. P., Miller, G. H., Lesnek, A. J., Crump, S. E., Thomas, E. K., Pendleton,
982 S. L., Cuzzone, J., Lamp, J., Zimmerman, S., Caffee, M., Schaefer, J. M., 2020a.
983 Deglaciation of the Greenland and Laurentide ice sheets interrupted by glacier advance
984 during abrupt coolings. *Quaternary Science Reviews* 229, 106091.
- 985 Young, N. E., Briner, J. P., Schaefer, J. M., Miller, G. H., Lesnek, A. J., Crump, S. E., Thomas,
986 E. K., Pendleton, S., Cuzzone, J., Lamp, J., Zimmerman, S., Caffee, M., 2020b. Reply to
987 Carlson (2020) comment on “Deglaciation of the Greenland and Laurentide ice sheets
988 interrupted by glacier advance during abrupt coolings”. *Quaternary Science Reviews* 240,
989 106354.
- 990 Young, N. E., Briner, J. P., Miller, G. H., Lesnek, A. J., Crump, S. E., Pendleton, S. L.,

- 991 Schwartz, R., Schaefer, J. M., 2021. Pulsebeat of early Holocene glaciation in Baffin Bay
992 from high-resolution beryllium-10 moraine chronologies. *Quaternary Science Reviews* 270,
993 107179.
- 994 Yu, S. Y., Colman, S. M., Lowell, T. V., Milne, G. A., Fisher, T. G., Breckenridge, A., Boyd,
995 M., Teller, J. T., 2010. Freshwater outburst from Lake Superior as a trigger for the cold
996 event 9300 years ago. *Science* 328(5983), 1262-1266.



998

999

1000 Fig. 1: Location of the study area with mapped moraine systems. A) Extent of the ice cover (light

1001 grey) in North America during the Last Glacial Maximum, modified from Dalton et al. (2020).

1002 B) Location of mapped moraine systems of the LIS discussed in this study, modified from

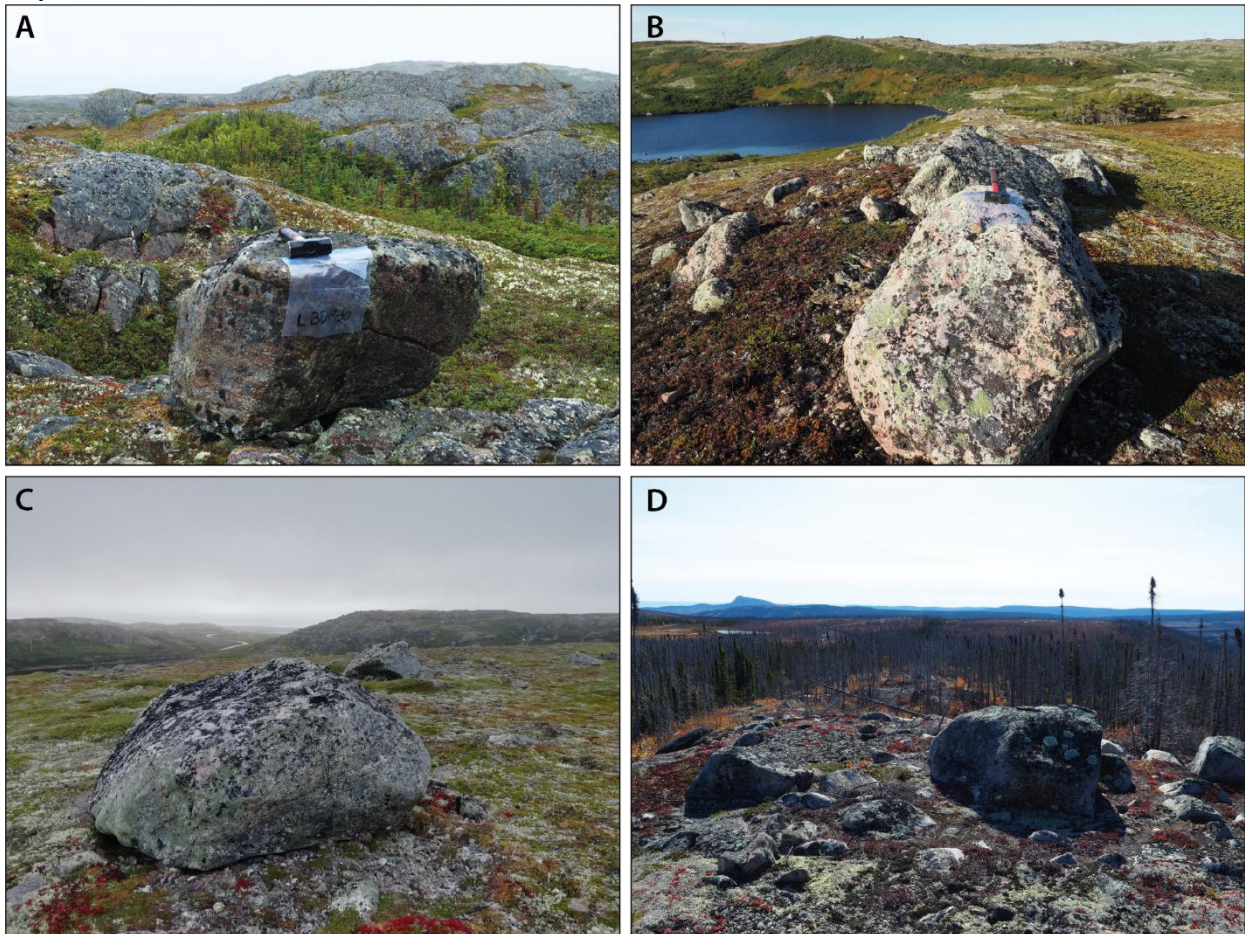
1003 Occhietti et al. (2011). NL : Newfoundland. (C) Easternmost Québec-Labrador and major

1004 moraine systems presented in this study. Sample location of our new cosmogenic ^{10}Be ages are1005 represented by diamonds and radiocarbon ^{14}C ages are represented by circles. All ages are

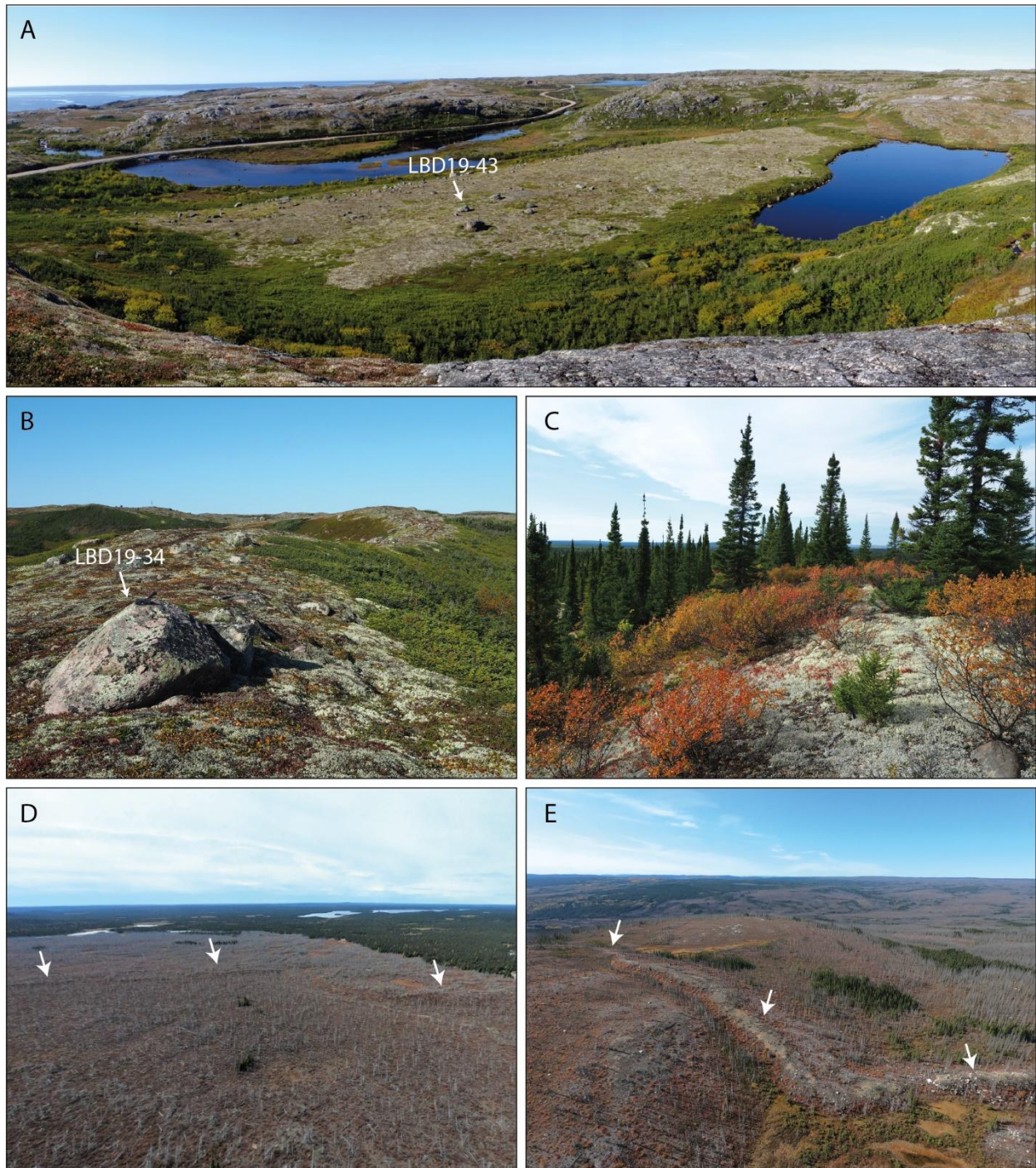
1006 reported in thousand years (ka). M1, M2, M3: unnamed moraine systems within and north of

Lake Melville, respectively from Syvitski and Lee (1997), Gebhardt et al. (2020) and Batterson

1007 et al. (1987). Red stars represent localities mentioned in the text. HV-GB: Happy Valley-Goose
1008 Bay.

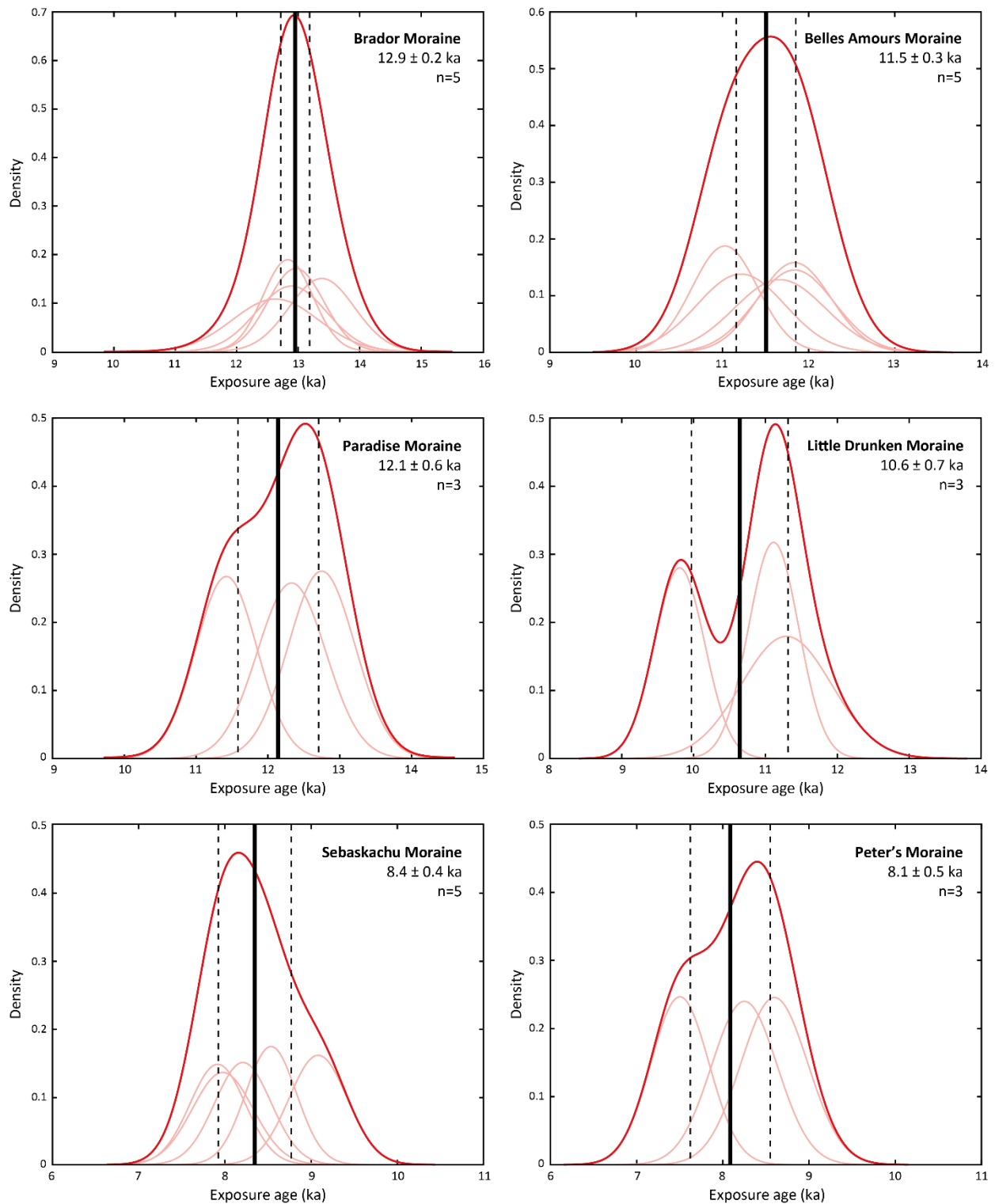


1009 Fig. 2: Examples of representative samples collected in easternmost Québec-Labrador. A)
1010 Sample LBD19-30 from a coastal erratic (14.1 ± 0.6 ka). B) Sample LBD19-36 from the Belles
1011 Amours Moraine (11.8 ± 0.4 ka). C) Sample LBD19-43 from the Brador Moraine (12.8 ± 0.5
1012 ka). D) LBD19-68 from the Sebaskachu Moraine (8.2 ± 0.4 ka).



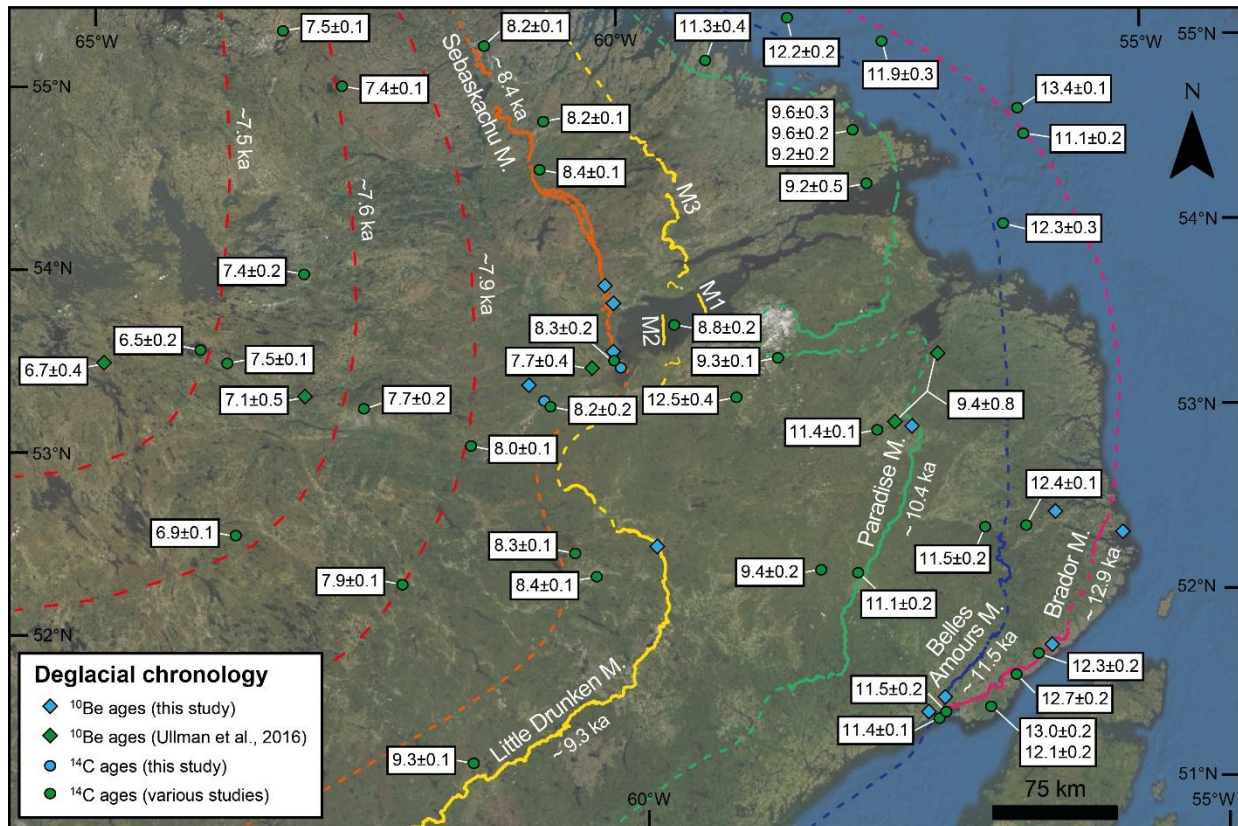
1014
 1015
 1016
 1017
 1018
 1019

Fig. 3: Photos of the major moraine systems of easternmost Québec-Labrador. A) View of the Brador Moraine, with representative sample LBD19-43 (12.8 ± 0.5 ka). B) View of the Belles Amours Moraine, with representative sample LBD19-34 (11.1 ± 0.5 ka). C) View of the Paradise Moraine. D) View of the Little Drunken Moraine (arrows). E) View of the Sebaskachu Moraine (arrows).

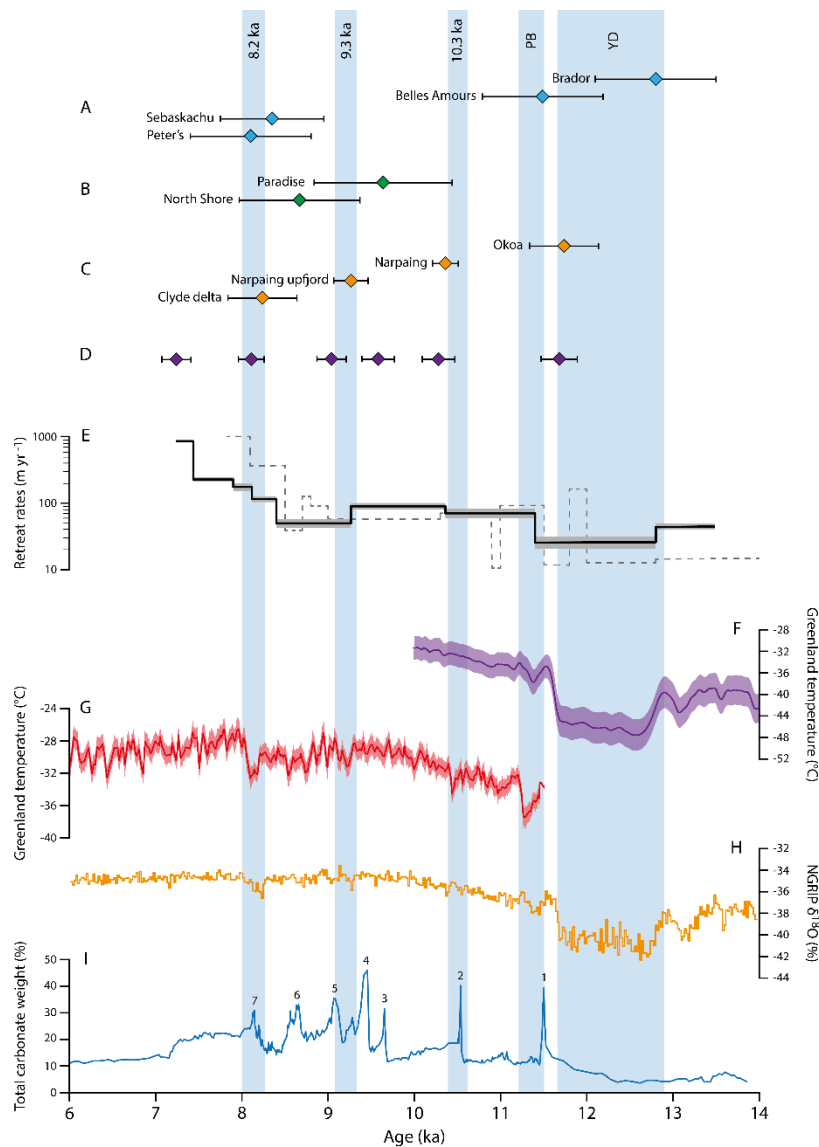


1020
 1021
 1022
 1023

Fig. 4: Probability distribution function (PDF) plots of ^{10}Be ages for moraine systems in easternmost Québec-Labrador, excluding outliers (see Results section and Table 1). The black and dashed lines represent the weighted average and the 1σ interval.



1024
 1025 Fig. 5: Previously published ages in easternmost Québec-Labrador. Cosmogenic ^{10}Be dating are
 1026 recalculated from Ullman et al. (2016). Radiocarbon ^{14}C dating are compiled from various
 1027 sources (Table 2). For ages from this study, the reader is referred to Fig. 1. All ages are reported
 1028 in thousand years (ka). Full lines represent mapped moraines and dotted lines represent potential
 1029 extension of these systems. Extension of the moraine systems and retreat isochrones of former
 1030 ice margin positions (i.e., 7.9, 7.6 and 7.5 ka) were tentatively drawn based on available
 1031 minimum- and maximum-limiting ages.



1032

1033 Fig. 6: (A) Exposure ages of moraine systems of easternmost Québec-Labrador from this study.
 1034 (B) Exposure ages of moraine systems of Labrador and Québec from Ullman et al. (2016). (C)
 1035 Exposure ages of moraine systems of LIS outlet glaciers on Baffin Island from Young et al.
 1036 (2020). Additionally, we used one site from Briner et al. (2007) and recalculated in Young et al.
 1037 (2013). (D) Composite record of Baffin Bay moraine deposition, from Young et al. (2021). (E)
 1038 Average retreat rates in southern Labrador reconstructed from this study (black line) with the
 1039 standard error of the mean (shading). Dashed dark gray line is from Dalton et al. (2020). Note
 1040 that retreat rates are represented in a logarithmic scale. (F) Greenland mean-annual temperatures
 1041 reconstructed using gas-phase $\delta^{15}\text{N-N}_2$ measurements (purple – $\pm 1\sigma$; Buizert et al., 2014). (G)
 1042 Greenland mean-annual temperatures reconstructed using gas-phase $\delta\text{Ar-N}_2$ measurements (red –
 1043 $\pm 2\sigma$; Kobashi et al., 2017). (H) $\delta^{18}\text{O}$ record from NGRIP project (orange; Rasmussen et al.,
 1044 2014). (I) Total carbonate weight chronology in core MD99-2236 collected on the Labrador
 1045 Shelf (blue; Jennings et al., 2015; Fig. 1). Vertical bars represent cold intervals discussed in the
 1046 text. YD: Younger Dryas; PB: Preboreal.

Table 1
Sample characteristics, AMS measurement results and ^{10}Be ages.

Sample no.	Latitude (DD)	Longitude (DD)	Altitude (m)	Quartz (g)	Carrier (mg)	$^{10}\text{Be}/^9\text{Be}$ (10^{-14})	Blank $^{10}\text{Be}/^9\text{Be}$ (10^{-14})	^{10}Be concentration (atoms g^{-1})	^{10}Be age (a)
Brador Moraine									12930 ± 240 (700)
LBD19-32	51.7933	-56.3825	162	6.7401	0.26480	3.08 ± 0.17	0.60 ± 0.09	64896 ± 3581	12613 ± 698
LBD19-33	51.7942	-56.3800	152	39.7256	0.48679	8.56 ± 0.27	0.59 ± 0.06	65264 ± 2062	12814 ± 406
LBD19-40	51.4997	-57.3684	138	9.6414	0.26606	4.09 ± 0.18	0.60 ± 0.09	64380 ± 2853	12873 ± 572
LBD19-42	51.4985	-57.3560	147	22.8433	0.51638	5.05 ± 0.17	0.61 ± 0.04	67092 ± 2662	13367 ± 557
LBD19-43	51.5075	-57.3217	142	28.7180	0.48375	6.37 ± 0.22	0.60 ± 0.07	64999 ± 2269	12945 ± 453
Belles Amours Moraine									11500 ± 340 (670)
LBD19-34	51.5021	-57.3821	167	13.9409	0.26473	5.14 ± 0.21	0.60 ± 0.09	57631 ± 2371	11163 ± 461
LBD19-35	51.5031	-57.3813	170	11.5690	0.26497	4.58 ± 0.20	0.60 ± 0.09	60894 ± 2636	11785 ± 512
LBD19-36	51.5044	-57.3812	168	28.1845	0.51652	5.64 ± 0.18	0.60 ± 0.07	61733 ± 6404	11972 ± 383
LBD19-38	51.5040	-57.3928	168	30.0281	0.51833	5.60 ± 0.21	0.60 ± 0.07	57695 ± 2181	11163 ± 423
LBD19-39	51.5044	-57.3926	168	17.8025	0.26348	6.46 ± 0.30	0.55 ± 0.06	58502 ± 2730	11334 ± 530
Paradise Moraine									12140 ± 560 (890)
LBD19-53	53.0460	-57.4695	193	30.0222	0.51350	10.37 ± 0.33	0.60 ± 0.07	111734 ± 3518	20805 ± 658 *
LBD19-54	53.0458	-57.4691	195	30.0476	0.51406	18.06 ± 0.57	0.60 ± 0.07	199659 ± 6300	37116 ± 1182 *
LBD19-56	53.0453	-57.4659	201	30.0862	0.51683	5.98 ± 0.22	0.60 ± 0.07	61830 ± 2303	11420 ± 427
LBD19-57	53.0449	-57.4638	199	16.2079	0.26464	6.64 ± 0.26	0.55 ± 0.06	66552 ± 2573	12328 ± 478
LBD19-58	53.0468	-57.4650	196	28.6727	0.50936	6.37 ± 0.22	0.60 ± 0.07	68549 ± 2484	12747 ± 463
Little Drunken Moraine									10640 ± 670 (960)
LBD19-63	52.4698	-59.8250	483	40.0595	0.52240	12.40 ± 0.42	0.59 ± 0.06	102959 ± 3451	14749 ± 496 *
LBD19-64	52.4699	-59.8256	492	40.1026	0.52521	11.44 ± 0.37	0.59 ± 0.06	94976 ± 3030	13483 ± 432 *
LBD19-65	52.4680	-59.8236	491	3.1706	0.21502	2.29 ± 0.12	0.53 ± 0.06	79756 ± 4431	11291 ± 629
LBD19-66	52.4678	-59.8234	490	40.0764	0.51965	8.58 ± 0.31	0.59 ± 0.06	69260 ± 2469	9803 ± 350
LBD19-67	52.4696	-59.8258	493	40.0306	0.51763	9.70 ± 0.30	0.59 ± 0.06	78693 ± 2475	11112 ± 350
Sebaskachu Moraine									8350 ± 420 (630)
LBD19-68	53.9088	-60.2298	351	25.6098	0.51636	4.40 ± 0.18	0.55 ± 0.06	51821 ± 2069	8204 ± 328
LBD19-69	53.9092	-60.2296	348	27.0470	0.51460	4.46 ± 0.18	0.55 ± 0.06	49764 ± 2021	7914 ± 322
LBD19-70	53.9091	-60.2296	348	25.4056	0.51304	4.76 ± 0.18	0.55 ± 0.06	56886 ± 2117	9082 ± 339
LBD19-71	53.9096	-60.2296	347	40.0772	0.52268	6.74 ± 0.23	0.59 ± 0.06	53605 ± 1847	8534 ± 295
LBD19-73	53.9108	-60.2297	347	26.7774	0.51674	4.43 ± 0.20	0.55 ± 0.06	50109 ± 2214	7973 ± 353
Peter's Moraine									8090 ± 460 (680)
LBD19-16	53.3786	-60.9337	172	21.9378	0.51781	3.35 ± 0.14	0.59 ± 0.05	43577 ± 2012	8250 ± 382
LBD19-17	53.3788	-60.9341	170	22.3020	0.51957	3.52 ± 0.14	0.61 ± 0.04	45240 ± 2040	8598 ± 389
LBD19-18	53.3770	-60.9374	163	30.9066	0.51881	2.75 ± 0.11	0.61 ± 0.04	35473 ± 1629	6827 ± 314 *
LBD19-19	53.3769	-60.9369	163	40.1043	0.51455	8.07 ± 0.28	0.59 ± 0.05	64171 ± 2544	12363 ± 492 *
LBD19-20	53.3785	-60.9322	163	20.6205	0.52079	2.92 ± 0.12	0.61 ± 0.04	39074 ± 1760	7500 ± 338
LBD19-28	52.5126	-56.2455	141	37.7807	0.51529	7.30 ± 0.23	0.59 ± 0.05	61183 ± 2293	12024 ± 452
LBD19-30	52.3696	-55.6632	140	35.0651	0.51566	7.86 ± 0.28	0.59 ± 0.05	71479 ± 2950	14104 ± 584
LBD19-31	52.3689	-55.6641	137	40.0454	0.51928	7.92 ± 0.26	0.59 ± 0.05	63520 ± 2475	12549 ± 491
LBD19-46	51.4780	-57.4756	75	28.3351	0.51864	4.63 ± 0.15	0.52 ± 0.04	50202 ± 1883	10632 ± 400
LBD19-74	53.8120	-60.1276	488	39.4430	0.51848	8.36 ± 0.26	0.53 ± 0.06	68788 ± 2570	9618 ± 360
LBD19-75	53.8136	-60.1272	488	40.8886	0.51544	11.73 ± 0.26	0.53 ± 0.06	94363 ± 3625	13268 ± 511
LBD19-84	53.5438	-60.1463	65	13.1005	0.26170	3.39 ± 0.17	0.60 ± 0.09	37259 ± 1919	7820 ± 404

1049 The ^{10}Be ages were calculated with the “LSDn” scaling scheme (Lifton et al., 2014), using the CRONUS-Earth online calculator version 3.0
1050 (Balco et al., 2008; <http://hess.ess.washington.edu/>) and the production rate calculated with the NENA calibration data set of Balco et al. (2009).
1051 The ^{10}Be AMS standard applied was the ASTER in-house STD-11 with a $^{10}\text{Be}/^9\text{Be}$ ratio of 1.19×10^{-11} (Braucher et al., 2015) and a ^{10}Be half-life
1052 of 1.387 ± 0.012 Ma (Chmeleff et al., 2010; Korschinek et al., 2010). A constant thickness of 2 cm and a rock density of 2.65 g cm^{-3} was applied
1053 for all samples. No erosion and no topographic shielding were accounted for in our calculations. Snow cover correction were not applied
1054 (Supplementary Material). The asterisks (*) mark the samples that are considered as outliers and were not included in the mean age calculations
1055 (in bold). Numbers in parentheses includes the production rate uncertainty.

Table 2
Radiocarbon and calibrated radiocarbon ages from material collected in easternmost Québec-Labrador.

Laboratory ID	Latitude (DD)	Longitude (DD)	Dated material	¹⁴ C a BP ± 1σ	Cal a BP ± 1σ	Source
LBD19-62	53.5192	-60.1469	<i>Hiatella arctica</i>	8155 ± 15	8460 ± 45	This study
LBD19-61	53.5192	-60.1469	<i>Mya truncata</i>	8150 ± 20	8460 ± 50	This study
LBD19-81	53.5192	-60.1469	<i>Mya truncata</i>	8120 ± 20	8430 ± 50	This study
LBD19-79	53.2596	-60.3774	<i>Mya arenaria</i>	7875 ± 120	8160 ± 150	This study
AA-58969	54.6166	-56.1761	Shell fragment	12 060 ± 60	13 390 ± 120	Jennings et al. 2015
BETA-16518	51.4900	-56.9800	Walrus bone	11 650 ± 160	12 980 ± 180	Harington et al., 1993
GSC-2825	51.6806	-56.6999	<i>Mya truncata</i>	11 300 ± 140	12 650 ± 160	Lowdon and Blake, 1979
SI-3139	53.2333	-58.5500	Gyttja	10 650 ± 290	12 480 ± 380	Lamb, 1980
GSC-3022	52.4500	-56.5300	Silty gyttja	10 500 ± 140	12 380 ± 120	Engstrom and Hansen, 1985
GSC-3014	54.1200	-56.6800	Foraminifera	11 000 ± 220	12 270 ± 300	Vilks et al., 1984
GSC-4283	51.7500	-56.5100	Gyttja	10 400 ± 120	12 260 ± 220	Grant, 1992
UCI-45371	55.3017	-58.1485	<i>Nuculana spp.</i>	10 925 ± 25	12 240 ± 160	Dalton et al., 2020
GSC-4175	51.4900	-56.9800	<i>Mya arenaria</i>	10 800 ± 120	12 050 ± 240	Grant, 1992
BETA-19574	55.1300	-57.4700	Mixed shells	10 710 ± 170	11 900 ± 300	Batterson et al., 1992
BETA-11697	51.5000	-57.2500	Shell	10 470 ± 120	11 530 ± 220	Dyke et al., 2003
SI-3350	52.5200	-57.0300	Gyttja	9985 ± 145	11 520 ± 200	Lamb, 1980
SI-3137	51.5166	-57.3000	Gyttja	9920 ± 110	11 410 ± 90	Lamb, 1980
SI-3348	53.0500	-57.7500	Silty gyttja	9910 ± 120	11 400 ± 100	Lamb, 1980
GX-6345	55.0833	-59.1667	Foraminifera	10 275 ± 225	11 270 ± 360	Barrie and Piper, 1982
GSC-3067	52.2700	-58.0500	Gyttja	9740 ± 170	11 110 ± 160	Blake, 1982
AA-16750	54.6200	-56.1800	<i>Yoldiella spp.</i>	10 155 ± 80	11 090 ± 170	Andrews et al., 1999
GSC-1453	54.6750	-57.8083	<i>Serripes Groenlandius</i>	9040 ± 230	9600 ± 320	Hodgson and Fulton, 1972
GSC-1453 (2L)	54.6750	-57.8083	<i>Serripes Groenlandius</i>	9030 ± 115	9570 ± 180	Hodgson and Fulton, 1972
WIS-1962	52.3000	-58.3700	Gyttja	8390 ± 80	9390 ± 45	King, 1985
WIS-1852	51.3170	-61.5100	Gyttja	8330 ± 110	9310 ± 110	King, 1985
WIS-1961	53.5800	-58.5800	Gyttja	8270 ± 80	9250 ± 100	King, 1985
GSC-1453 (1L)	54.6750	-57.8083	<i>Serripes Groenlandius</i>	8750 ± 150	9220 ± 200	Hodgson and Fulton, 1972
SI-1739	54.4000	-57.7167	Gyttja	8255 ± 400	9190 ± 480	Jordan, 1995
TO-200	53.7100	-59.5767	<i>Nuculana Minuta</i>	8380 ± 90	8750 ± 170	Vilks et al., 1987
WIS-1850	52.3167	-60.3833	Gyttja	7620 ± 120	8420 ± 110	King, 1985
TO-1123	54.5500	-60.7833	<i>Nuculana spp.</i>	8080 ± 60	8380 ± 120	Awadallah and Batterson, 1990
WIS-1963	52.4500	-60.5667	Basal gyttja	7510 ± 80	8310 ± 50	King, 1985
GSC-2970	53.5250	-60.1500	<i>Balanus hameri</i>	8000 ± 100	8290 ± 150	Lowdon and Blake, 1980
BETA-28885	54.8167	-60.7333	<i>Portlandia</i>	7950 ± 90	8240 ± 140	Awadallah and Batterson, 1990
GSC-1254	53.2583	-60.7458	<i>Pelecypod</i>	7890 ± 150	8180 ± 180	Lowdon and Blake, 1975
TO-5695	55.2202	-61.2873	<i>Mesodesma arctatum</i>	7880 ± 70	8170 ± 120	Dyke et al., 2003
WIS-1855	53.0500	-61.4833	Gyttja	7150 ± 80	7970 ± 50	King, 1985
GSC-3661	52.3000	-62.1167	Gyttja	7080 ± 110	7890 ± 40	King, 1985
WIS-1960	53.2667	-62.4500	Lake sediments	6810 ± 100	7660 ± 90	King, 1985
WIS-1849	53.5000	-63.7000	Gyttja	6620 ± 110	7500 ± 80	King, 1985
GSC-3241	55.3333	-63.3000	Gyttja	6600 ± 100	7490 ± 80	Lamb, 1985
GSC-1592	54.0000	-62.9900	Mosses	6560 ± 200	7440 ± 180	Lowdon and Blake, 1973
GSC-3252	55.0330	-62.6330	Gyttja	6520 ± 150	7410 ± 110	Lamb, 1985
GSC-3640	52.5700	-63.6000	Gyttja	6050 ± 90	6910 ± 110	King, 1985
I-728	53.5800	-63.9500	Basal peat	5275 ± 250	6490 ± 240	Morrison, 1970

1058 The AMS ¹⁴C ages were calibrated within the age-depth modelling process, using the online software Calib 8.2 with the Marine20 (Heaton et al.,
1059 2020) and IntCal20 (Reimer et al., 2020) radiocarbon age calibration curves. A local reservoir correction (ΔR) of -2 ± 69 was used to account for
1060 the regional offset of the world ocean ¹⁴C age, as determined by McNeely et al. (2006).